NASA CR-54785
PWA-2713

FIRST QUARTERLY REPORT

BRAYTON-CYCLE TURBOMACHINERY ROLLING-ELEMENT BEARING SYSTEM

prepared for
National Aeronautics and Space Administration

October 1965

Contract NAS3-7635

National Aeronautics and Space Administration
Lewis Research Center
21000 Brookpark Road
Cleveland, Ohio
Lloyd W. Ream

Prepared by H Means H. Means, Project Engineer

Approved by Peter Bolan P. Bolan, Program Manager

Pratt & Whitney Aircraft DIVISION OF UNITED AIRCRAFT CORP.
EAST HARTFORD • CONNECTICUT

FOREWORD

This report describes the progress of work conducted between July 2 and October 2, 1965 by the Pratt & Whitney Aircraft Division of United Aircraft Corporation, East Hartford, Connecticut on Contract NAS3-7635, Brayton-Cycle Turbomachinery Roller-Contact Bearings, for the Lewis Research Center of the National Aeronautics and Space Administration. The objective of the program is to design and demonstrate performance of a rolling-element bearing system for the Brayton-cycle turbomachinery being developed on Contracts NAS3-4179 and NAS3-6013.

TABLE OF CONTENTS

LIST OF FIGURES

LIST OF FIGURES (Continued)

I. SUMMARY

This report describes the work completed during the first three months of a design and experimental program formulated to investigate the potential of oil-lubricated rolling-element bearings for Brayton-cycle space power machinery. The technical progress, the work accomplished and the program status for the first quarterly period from July 2 through October 2, 1965 are covered.

A basic bearing-seal lubrication, scavenge, and separation system concept adaptable to the turbomachinery being developed on Contracts NAS3-4179 and NAS3-6013 was evolved. The selected concept is versatile and permits alternate component configurations to be incorporated if they demonstrate superior performance in the component test program. Mechanical design work was initiated on both the turbine-compressor and the turboalternator to replace the gas bearing rotor support system with an oil-lubricated rolling-element bearing system. A detailed design analysis was made to define the geometry of the rolling-element bearings for the turbine-compressor. Lubricant evaluations were initiated to form a basis for selection of the optimum lubricant for the Brayton-cycle turbomachinery. The effects of oil contamination of the Brayton-cycle working fluid (argon) were studied to establish limiting oil contamination criteria. An oil adsorber program was started with the objective of determining the performance capabilities and design parameters of various types of adsorbers for separating oil from argon.

II. INTRODUCTION

In the application of the Brayton cycle to space power sources, two types of rotor support systems are being considered and evaluated by the National Aeronautics and Space Administration. In one case, the rotating components are supported by gas bearings and the cycle working fluid is used as lubricant and bearing coolant. In the other case, the rotors are supported by rolling-element bearings which are lubricated and cooled by oil.

The specific Brayton-cycle machinery considered in this program consists of a turbine-driven compressor and a turbine-driven alternator. These units are being designed and constructed utilizing gas bearings under Contracts NAS3-4179 and NAS3-6013. The gas bearing version of this machinery is shown in Figure 1. The cycle flow enters the compressor at 76°F through the inlet duct around the housing which contains a thrust bearing and a radial bearing. The argon is compressed in the six-stage axial-flow compressor and then flows through the radial diffuser exit scroll and ducting. The argon is heated to 1490°F outside of the unit and is returned to the turbine inlet ducting and scroll. A second radial gas bearing is located between the compressor exit and turbine inlet. The argon flows through the single-stage axial-flow turbine which drives the compressor at 50,000 rpm. It then exhausts through the exit ducting which connects to the two-stage alternator-drive turbine. The 4-pole alternator is driven at 12,000 rpm and is supported by bearings on each side. After passing through the alternator-drive turbine, the argon exhausts through the exit scroll and ducting. It is cooled outside of the machinery and returned to the compressor inlet.

The vast majority of Brayton-cycle powerplants in use in the world today employ rolling-contact oil-lubricated bearings. In the application of Brayton-cycle machinery to the space environment, several significant questions require investigation to determine if rolling-element bearings can provide a satisfactory rotor support system for this application:

1) Can rolling-element bearings provide the endurance capability with the high reliability required in space applications for a nominal mission time of 10,000 hours?

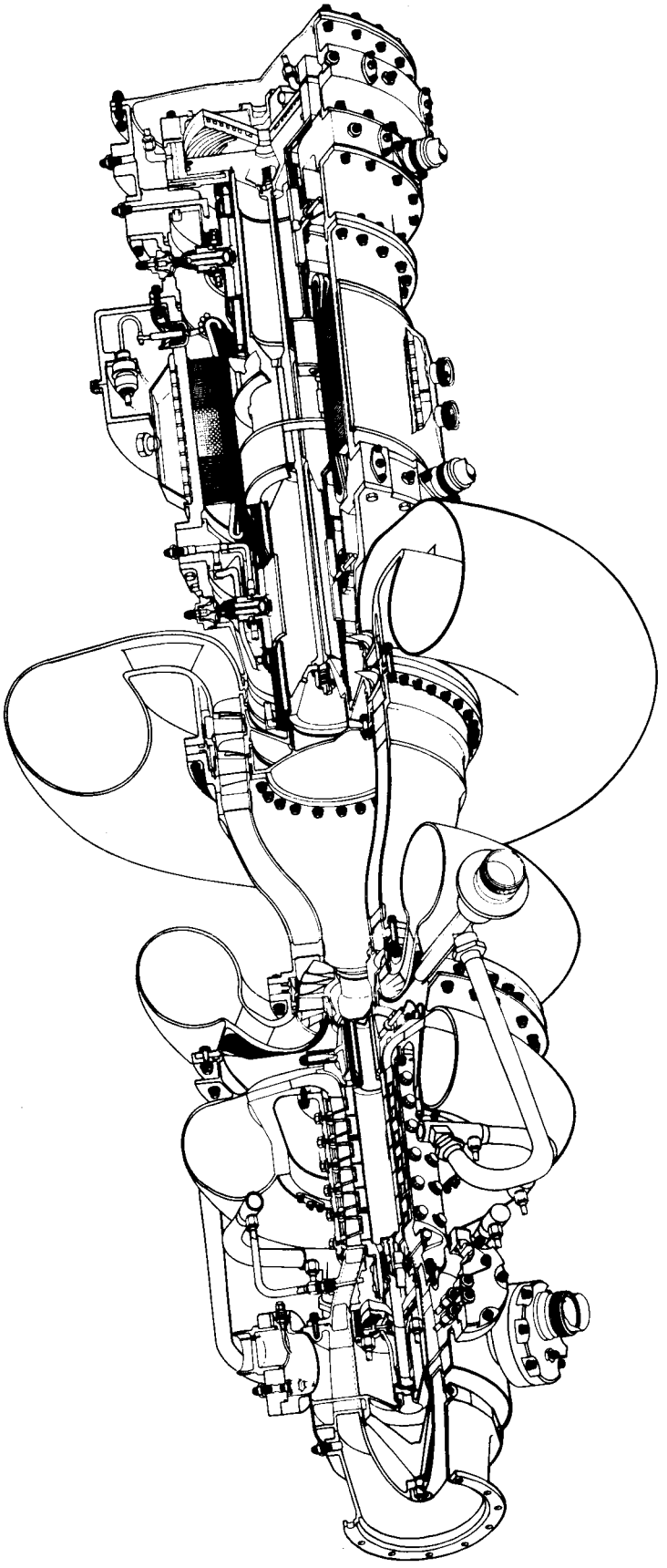

Figure 1 Brayton-Cycle Turbomachinery

Contracts NAS3-4179 and NAS3-6013

2) Can the lubricant be cooled and circulated in a zero-gravity environment?

3) Can the lubricant system and bearing cavities be sealed with low parasitic power losses by components with the required life capability?

4) Can the lubricant be prevented from contaminating the cycle working fluid (argon)?

The purpose of this program is to design and demonstrate the performance of a rolling-element bearing system for the turbine-compressor and turboalternator being developed under Contracts NAS3-4179 and NAS3-6013. The components of this rolling-element bearing system are bearings, seals, lubrication system and gas cleanup system. The work consists of the following four phases:

1) Design of a rolling-element bearing system that retains components of the turbine-compressor and turboalternator (designed under Contracts NAS3-4179 and NAS3-6013) to as great an extent as practical with no alteration in aerodynamic design. The shaft support system is intended to achieve low parasitic losses commensurate with high reliability for the full mission life.

2) Design and fabrication of component test rigs.

3) Conduct bearing, seal, scavenge separator and adsorber performance tests.

4) Conduct a pilot endurance demonstration of the rolling-element bearing system.

Although the rolling-element bearing system encompasses the turboalternator as well as the turbine-compressor, only the rolling-element bearing system components for the turbine-compressor will be investigated experimentally. The separator, which is an integral part of the turboalternator, will be evaluated in a separate test rig as will the residual oil adsorber.

III. ROLLING-ELEMENT BEARING LUBRICATION SYSTEM

The objective of the lubrication system for Brayton-cycle turbomachinery is to provide proper lubrication of the bearings and seals and prevent contamination of the basic cycle working fluid, argon, during development testing, ground checkout and orbital operation. Since the lubrication system must function in a gravity-free environment as well as under gravity, centrifugal forces are employed to circulate the necessary fluids and to separate the oil and argon. The lubricant is used to cool the bearings and a small amount lubricates surfaces within the bearings where rolling or sliding occur. A combination of labyrinth and face seals is used to separate the fluids in the bearing compartments from the main cycle gas.

A schematic diagram of the selected lubrication system is presented in Figure 2. Oil is supplied from an accumulator which feeds a rotating pool of oil inside the turboalternator shaft. The oil enters the system through a tube which forms a scoop in the rotating reservoir. This configuration can be visualized more readily by Figure 3 which shows the mechanical arrangement of this scoop tube in relation to the turboalternator and centrifugal separator. This type of stationary scoop develops a fairly high head when totally immersed in the pool of oil rotating at a linear speed of 50 feet per second. When the scoop opening is only partially immersed in oil, the head is lost. Therefore, if the reservoir contains too little oil and the oil level is below the scoop, oil flows from the pressurized accumulator into the system. If the oil level rises above the scoop, the pumping action forces oil back into the reservoir, and the result is a rotating reservoir with essentially a constant inventory. This system permits a fairly wide range of acceptable accumulator oil pressure for proper operation. Since the turboalternator speed is maintained at 12,000 rpm and since the oil level in the rotating reservoir is fixed, a given head is maintained at the bottom of the reservoir. Holes are located at the bottom of the reservoir which meter oil flow to the turboalternator bearings.

The oil cools the bearings by passing through slots in the inner race and oil in the form of mist in the bearing compartment provides lubrication. The oil cools the rotating face seal plate after leaving the bearing. In Figure 2, oil-lubricated wet face seals are indicated but

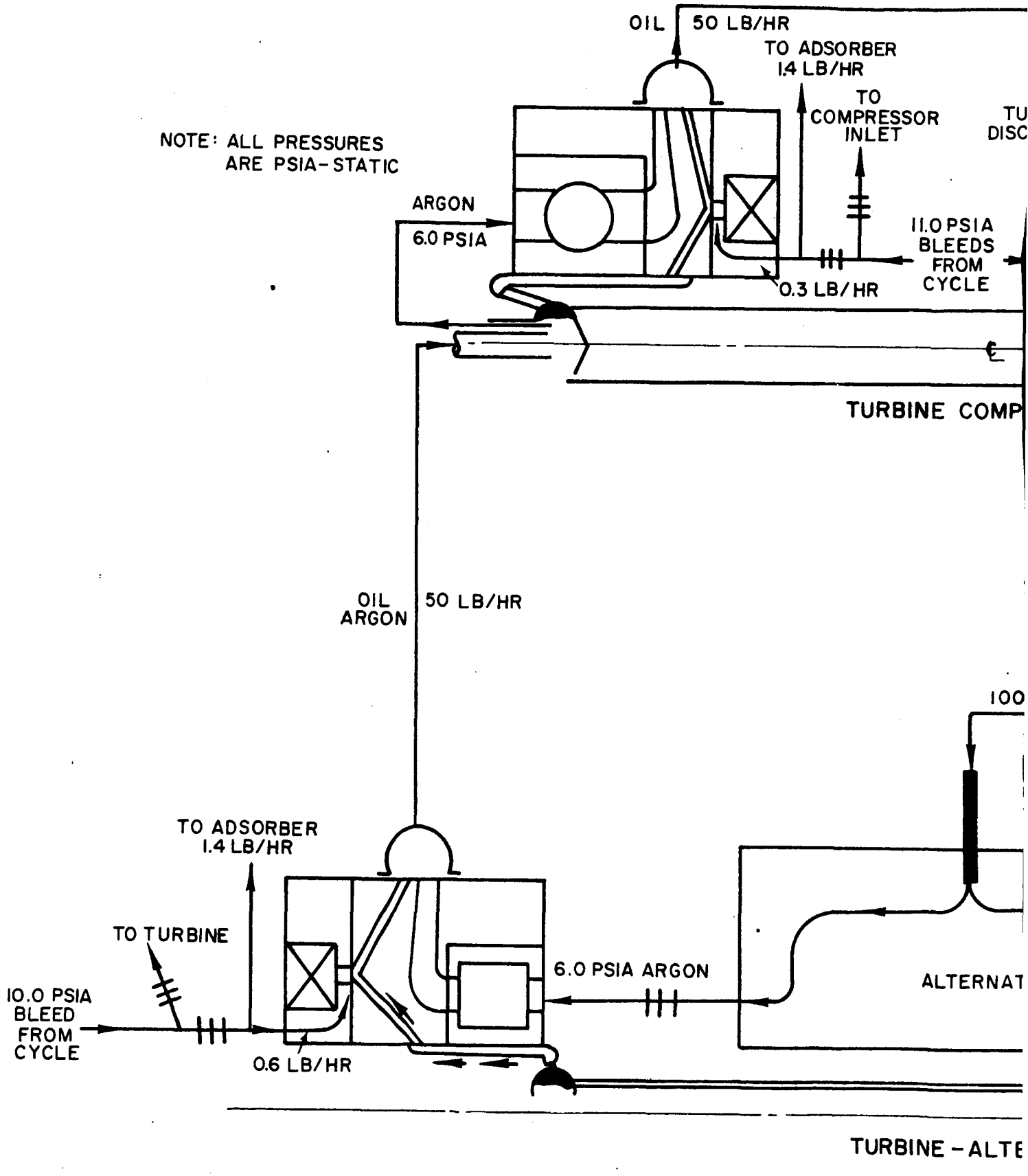

Figure 2 Schematic of Brayton-Cycle Rolling-Element Bearing System

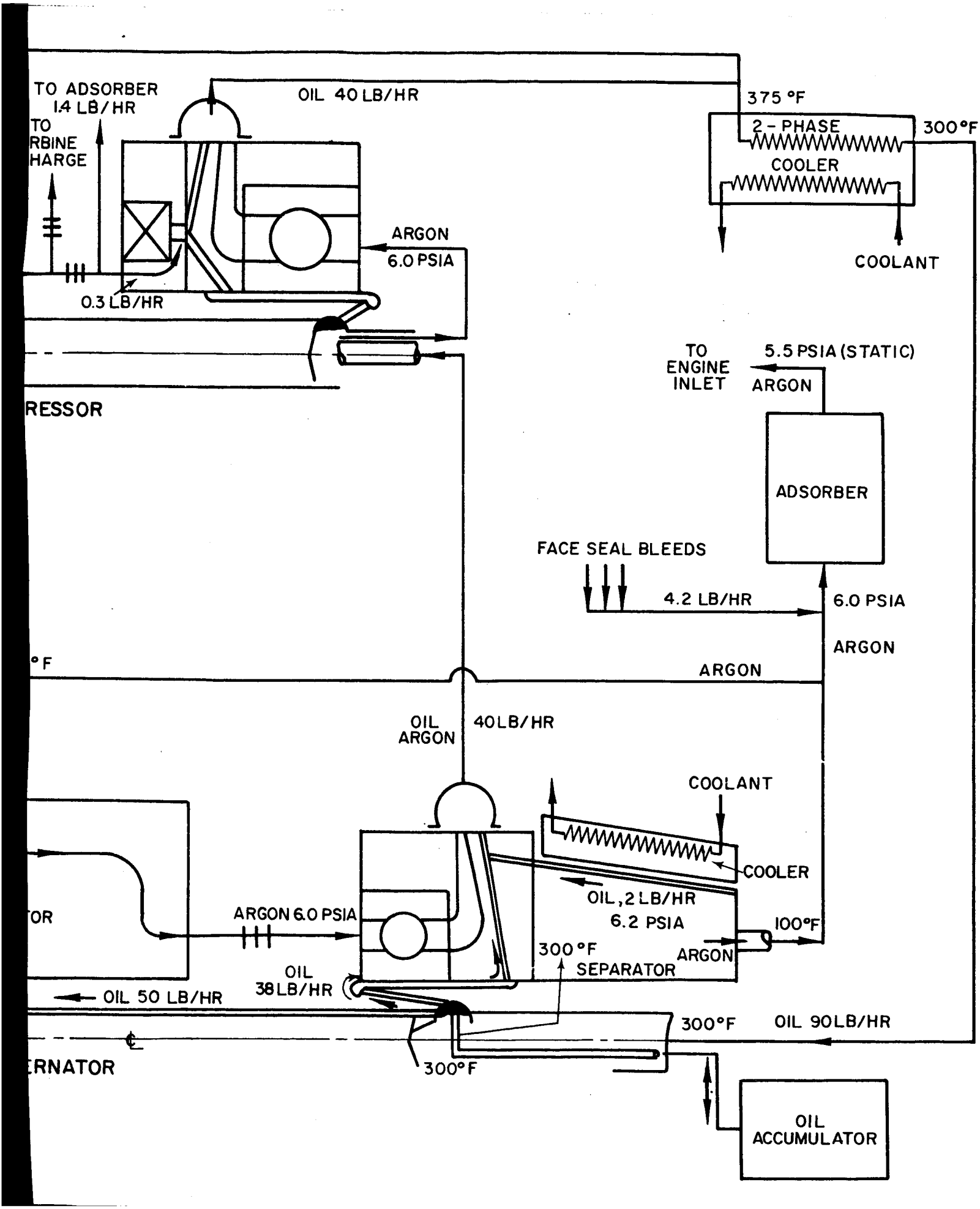
TO ADSORBER
1.4 LB/HR
TO
RBINE
HARGE
OIL 40 LB/HR
375 °F
2 - PHASE
COOLER
300°F
COOLANT
ARGON
6.0 PSIA
0.3 LB/HR
RESSOR
TO
ENGINE
INLET
5.5 PSIA (STATIC)
ARGON
ADSORBER
FACE SEAL BLEEDS
4.2 LB/HR
6.0 PSIA
ARGON
°F
ARGON
OIL
ARGON
40LB/HR
COOLANT
COOLER
OR
ARGON 6.0 PSIA
OIL, 2 LB/HR
6.2 PSIA
100°F
300 °F
ARGON
SEPARATOR
OIL
38LB/HR
OIL 50 LB/HR
300°F
OIL 90LB/HR
ERNATOR
300°F
OIL
ACCUMULATOR

dry face seals could be used. The seal plate would still require oil cooling but with dry face seals the oil passages would pass radially through the plate. Two labyrinth seals are provided on the gas side of the face seals and high pressure gas is bled from the compressor and fed between these labyrinth seals. Some of this gas leaks back to the main cycle stream and some leaks into the bearing compartment. A small flow of argon is bled from the area just upstream of the face seal to the adsorber. The object of this flow is to carry any oil which weeps past the face seal to the adsorber.

The back side of the face seal plate shown in Figure 2 includes vanes to provide a small centrifugal pump to force the argon out of the bearing compartment. The forward (Number 1) bearing compartment of the turbine-compressor is scavenged in a similar manner and this section is shown in Figure 4. The oil leaving the seal plate has rotational velocity, and two techniques are being considered to recover this energy. In one case the seal plate would include a cavity where the oil would form a rotating pool and a stationary scoop would act as an oil pump, as shown in Figure 4. The oil and argon would leave the bearing compartment through separate pipes. In the other case, the oil would be mixed with the argon leaving the impeller and the two fluids would flow in a single pipe. This second scheme would be adapted to the bearing cavity shown in Figure 4 by omitting the scoop and seal plate extension and replacing them with a pump discharge collector of conventional shape.

The pressure rise in the argon developed by the seal plate impeller is low. Therefore, the gas and oil system is connected in series so that pumping action of the turbine-compressor seal plate can be added to the turboalternator pressure rise to move the argon through the system. The oil and argon which leave the turboalternator bearing compartments are piped to the inside of the turbine-compressor shaft. The centrifugal field within the shaft separates most of the oil from the argon and the oil passes under the bearing and through the seal plate as in the turboalternator. The argon flows out the end of the shaft carrying some oil mist with it and then through the bearing to the seal plate impeller. The oil and argon are pumped out of the bearing compartment as before.

In the process of cooling the bearings and seals, the oil and argon in the bearing compartment are heated to about 375°F. As shown in Figure 2, this mixture passes through a liquid-cooled heat exchanger and is returned to the inside of the turboalternator shaft and the centrif-

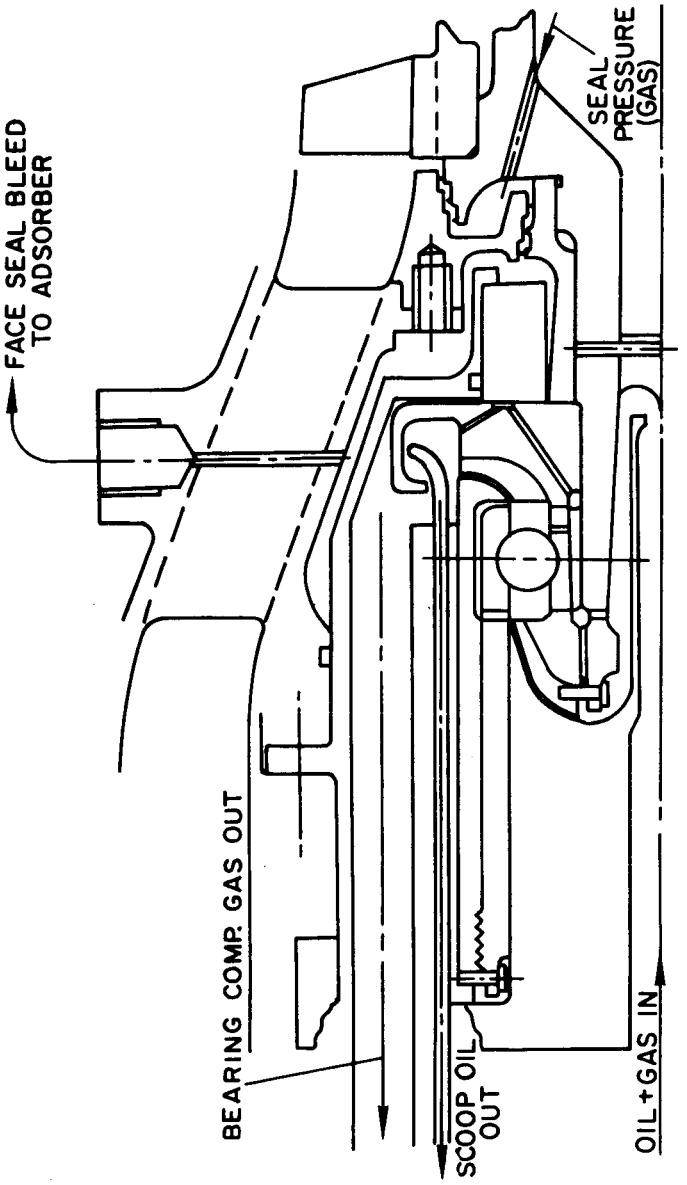

Figure 4 Preliminary Arrangement of Turbine-Compressor Bearing Cavity with Scoop Scavenge Concept

ugal separator. At this point in the lubrication system the centrifugal separator, mounted on the turboalternator shaft and shown in Figure 3, centrifuges oil from the oil-argon mixture to the outer periphery of the rotating gauze-like metallic mesh where the separated oil flows along the tapered housing to rejoin the turboalternator oil flow. The metallic mesh permits gas to pass but the oil droplets hit the mesh and acquire rotational velocity. Since the oil particles are denser than the gas they are centrifuged to the outer wall. In order to reduce the amount of oil vapor leaving the system and to assist the separation process, the centrifugal separator is cooled by a static cooling jacket surrounding the separator. The cool argon containing a small amount of oil vapor passes through the molecular sieve (adsorber) where any oil retained in the argon is adsorbed and the clean argon is returned to the cycle. Some argon is recirculated through the lubrication system and the argon re-enters the system through the alternator cavity. Labyrinth seals separate the bearing compartments from the alternator and the argon flowing through these seals limits the amount of oil which can flow into the alternator cavity.

The gas pressure level in the bearing cavities is determined by the pressure drop of the argon passing through the adsorber. The total flow through the adsorber, in turn, is dependent upon the argon leakage through the seals. Therefore, the bearing compartment pressure level will build up to a pressure somewhat higher than the adsorber discharge pressure. For the leakages anticipated, the bearing compartment pressure is estimated to be approximately 0.5 psi above the adsorber discharge pressure.

IV. TURBINE-COMPRESSOR DESIGN

The basic turbine-compressor design task of this program is to adapt a rolling-element bearing system that can be used as an alternate to the gas bearing system which is presently being developed under Contract NAS3-4179. The overall design objectives and considerations are, 1) to use a bearing, seal, and lubrication system that provides endurance capability with a high degree of reliability for a mission time of 10,000 hours, 2) to use a bearing, seal, and lubrication system that has acceptable parasitic losses, and 3) to evolve a mechanical design that utilizes the existing aerodynamics with minimum mechanical alterations.

A. Mechanical Arrangement

The first consideration in the mechanical design of the turbine-compressor rolling-element bearing system is the location of the bearings. The gas bearings designed under Contract NAS3-4179 are located upstream of the compressor and between the compressor and the turbine. The compressor inlet is also a logical location for one of the rolling-element bearings. The shaft diameter required between the compressor and turbine to maintain shaft stiffness would require a large bearing operating at high speed with high parasitic loss. Also, seals would be required on both sides of the bearing with the bearing located between the compressor and turbine. Therefore, a straddle-mounted arrangement with bearings outboard of the compressor and turbine was selected. A preliminary drawing of this arrangement is shown in Figure 5.

The space available at the turbine discharge is limited. The exit duct has been revised to provide more space and to provide a bearing mount arrangement with a long thermal path from the hot turbine discharge gas. The turbine (Number 2) bearing is mounted on a shaft extension to aid in the thermal isolation of the bearing compartment. A coupling has been introduced in the compressor end of the shaft to permit fabrication and assembly of the units.

B. Critical Speed Analysis

Analysis of the rotor system is particularily important to determine the resonant modes of vibration (critical speeds). The results of the analysis of a preliminary configuration similar to Figure 5 is presented in Figure 6 for various bearing support stiffnesses. The results are

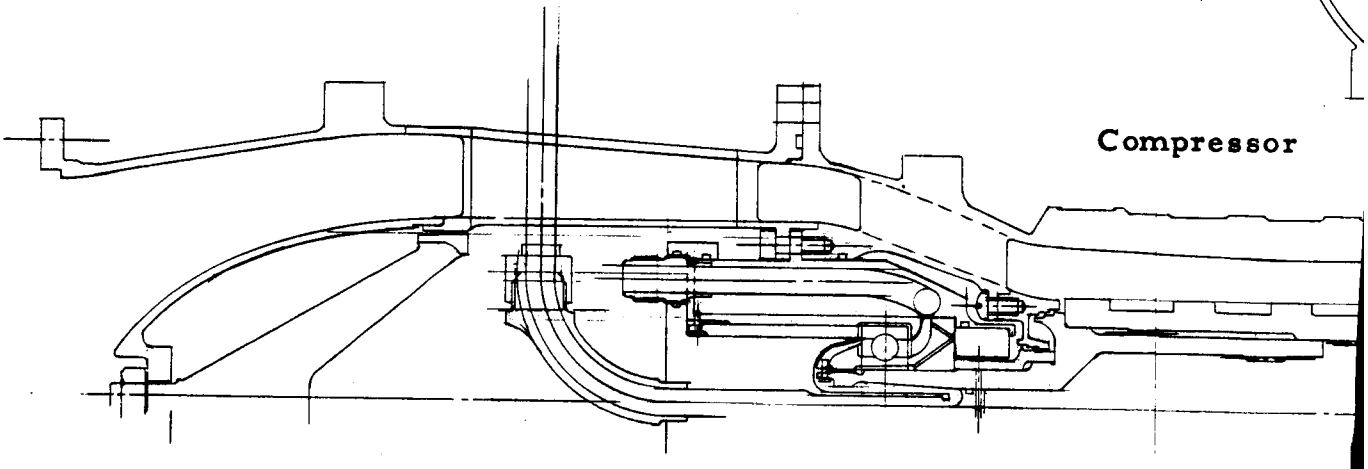

Figure 5 Brayton-Cycle Turbine-Compressor. Preliminary Rolling-Contact Bearing Arrangement

2

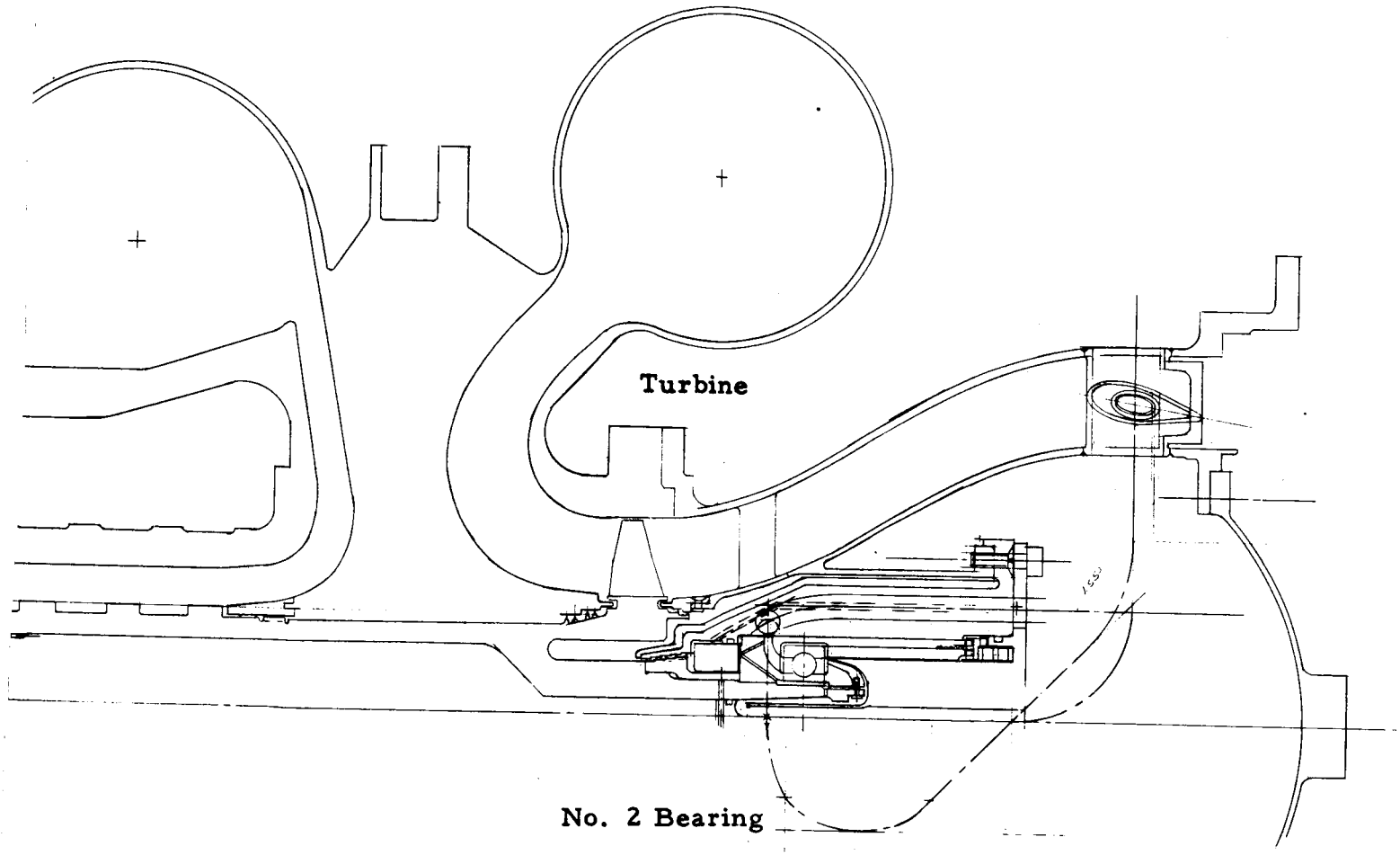

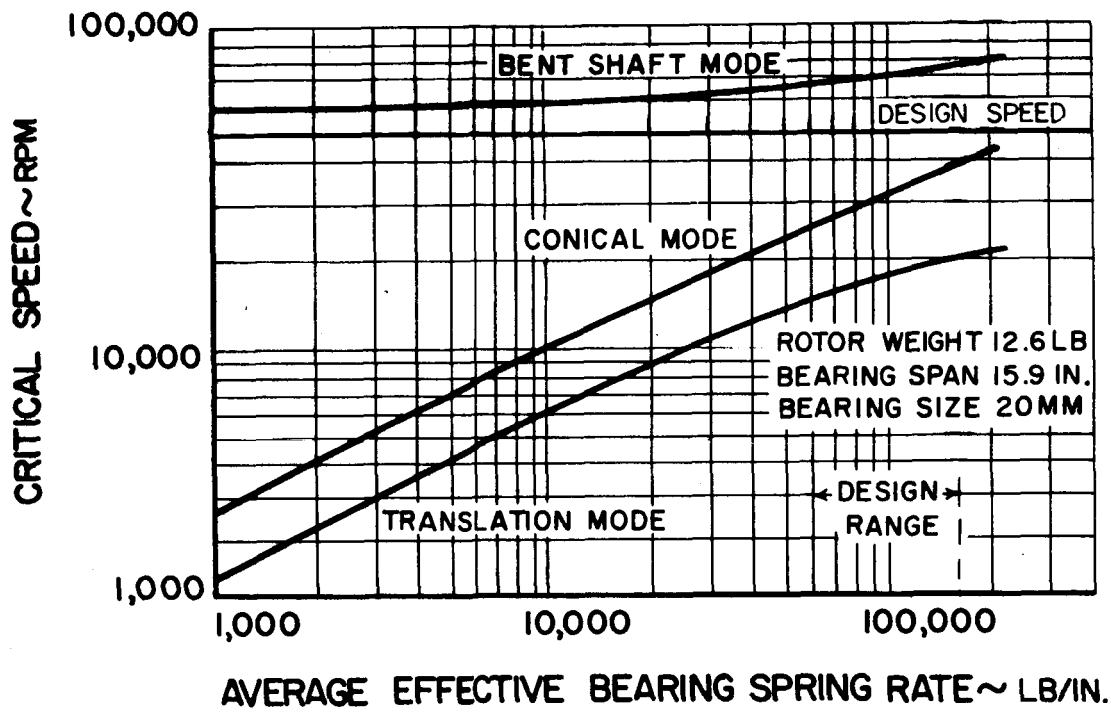

Figure 6 Preliminary Turbine-Compressor Critical Speeds

also presented in the following table for bearing and mount stiffnesses in the range of interest:

Turbine-Compressor Critical Speeds

Support stiffness, pounds/inch	50,000	100,000	200,000
First mode (translation), rpm	13,934	18,435	21,810
Second mode (conical), rpm	24,500	33,030	44,100
Third mode (bent shaft), rpm	65,700	74,200	83,500

There are two essentially rigid-body critical speeds below the design operating speed of 50,000 rpm and a bent-shaft (free-free) critical speed above the design speed. In order to provide reasonable margin above the design speed, a bent-shaft critical speed above 70,000 rpm was selected as a design criterion. To meet this criterion the stiffness of the bearing and its support should be above 60,000 pounds/inch. Also an upper limit of 40,000 rpm was selected as the design criterion for the rigid-body critical speed which restricts the bearing and mount system spring rate to less than 160,000 pounds/inch.

C. Bearing Analysis and Design

The basic objective in the design of bearings for the Brayton-cycle turbine-compressor is to provide a rotor support system for the hardware designed under Contract NAS3-4179 with minimum alteration of the compressor, turbine, or scrolls. The performance goal is to evolve a design that would achieve a B_1 failure rate of 1.0 per cent or lower for 10,000 hours with minimum power consumption and wear.

The shaft diameter between the turbine and the compressor by necessity is approximately 50 mm which would result in a bearing DN (the linear speed of a bearing is usually defined as the product of the bore diameter, D, in millimeters and the shaft rotational speed, N, in rpm) of at least 2.5×10^6 at the design speed of 50,000 rpm, if a bearing were located between the turbine and compressor. To avoid this unreasonably high linear speed, a straddle-mounted concept was selected and the choice of bearing diameter became somewhat independent of shaft size. To preclude skidding which could occur in a lightly-loaded

high-speed application such as this, the choice was made to incorporate two ball bearings to support the rotor, thrust-loaded against each other by a spring, rather than a ball bearing at one end and a roller bearing at the other. A preliminary drawing of the turbine-compressor bearing arrangement is presented in Figure 5.

Having established the rotor-bearing arrangement configuration and envelope limitations, the selection of bearing size and geometry depended on three major factors: fatigue life, friction losses and skidding tendencies. In designing for long fatigue life, large bearings are normally selected. Fatigue life is usually improved with tight race curvatures and, in the case of pure thrust loading, high design contact angle. Unfortunately the skidding tendencies are increased by these factors as well. Also, large sizes, large contact angles and tight curvatures result in high levels of heat generation. Thus, the final bearing design is a compromise between long fatigue life on the one hand and low skidding characteristics and frictional power loss on the other.

Studies were conducted using digital computer techniques to evaluate the tradeoffs between bearing life, skidding margin and geometry. Power consumption, lubrication, installation, fabrication, and metallurgical factors were also considered. The life of bearings of various diameters was examined at the design speed of the turbine-compressor (50,000 rpm) with a combined radial and thrust load. A 20-pound radial load was selected as representative of the maximum radial force anticipated due to mechanical unbalance in the rotor at the end of 10,000 hours of operation. The minimum thrust load to assure operation without skidding was employed for each bearing size, and this value of thrust increases as the bearing size is increased. The results of these calculations are summarized in Figure 7 which presents bearing life as a function of size. In addition, the effects of misalignment of the shaft from 0 to 0.0005 radians on bearing life are included. While misalignments as large as 0.0005 radians are not anticipated, the bearing life would not be affected appreciably by such a misalignment. Bearing life increases as the bearing size is reduced, primarily because the linear speed of the bearing is reduced and the skid-free thrust load is reduced.

The predicted friction heat generation of various size bearings with mist

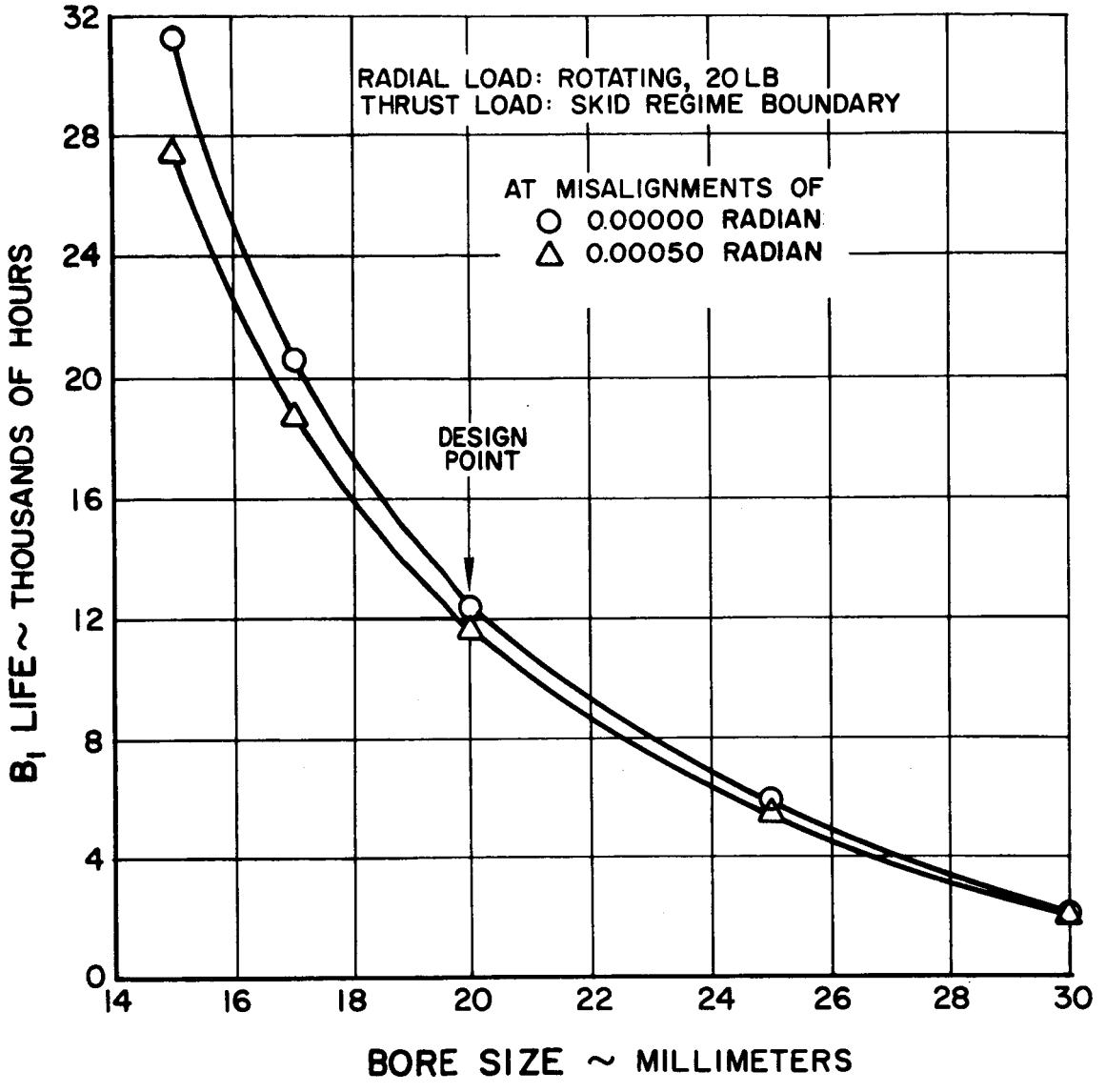

Figure 7 Bearing B_1 Life vs Bore Size

lubrication is presented in Figure 8. The lowest friction losses occur with the smallest bearing. Therefore, for a design with a thrust load to avoid skidding, the smallest bearings provide the longest life and lowest heat generation. The mechanical design of the bearing compartment indicates that difficulty will be encountered in providing the lubrication and cooling system for bearings of less than 20 mm bore; therefore, a 20 mm bore diameter bearing was selected.

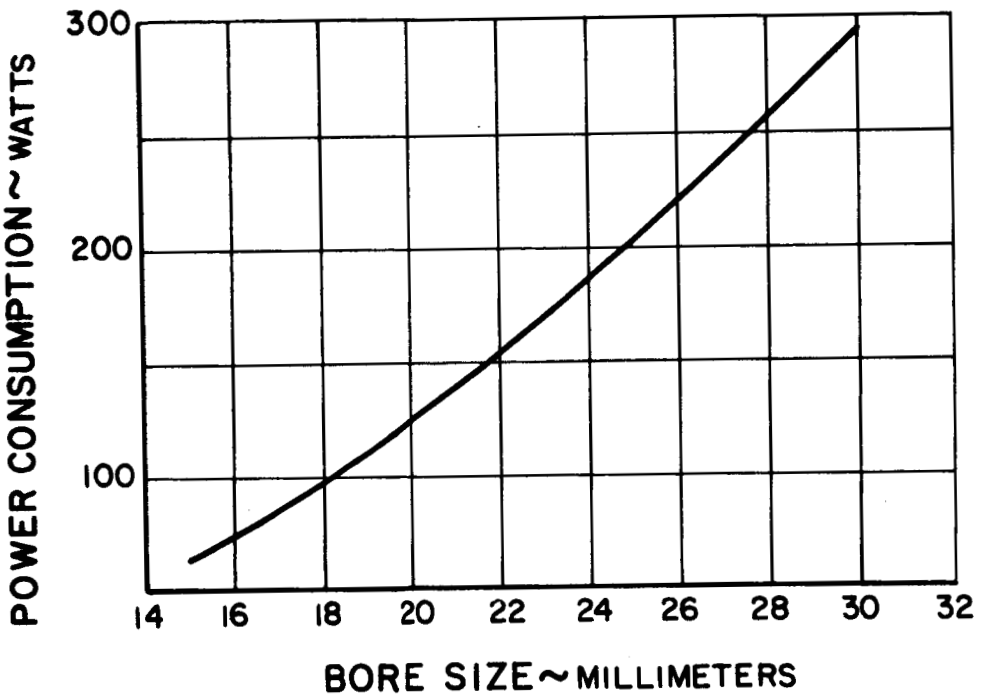

Figure 8 Power Consumption vs Bore Size

The results presented in Figure 7 include a ball diameter variation consistent with the standard extra light series of bearings. The study included an examination of various ball diameters for 20 mm bore bearings and the results are presented in Figure 9. The life of the bearing improves as the ball diameter is reduced as a result of smaller centrifugal effects and the associated lower skid-free thrust loads. The 0.250-inch diameter ball was selected for this application to avoid excessive sensitivity to misalignment and internal clearance variations. Also, smaller balls would introduce difficulty in the mechanical design of the retainer.

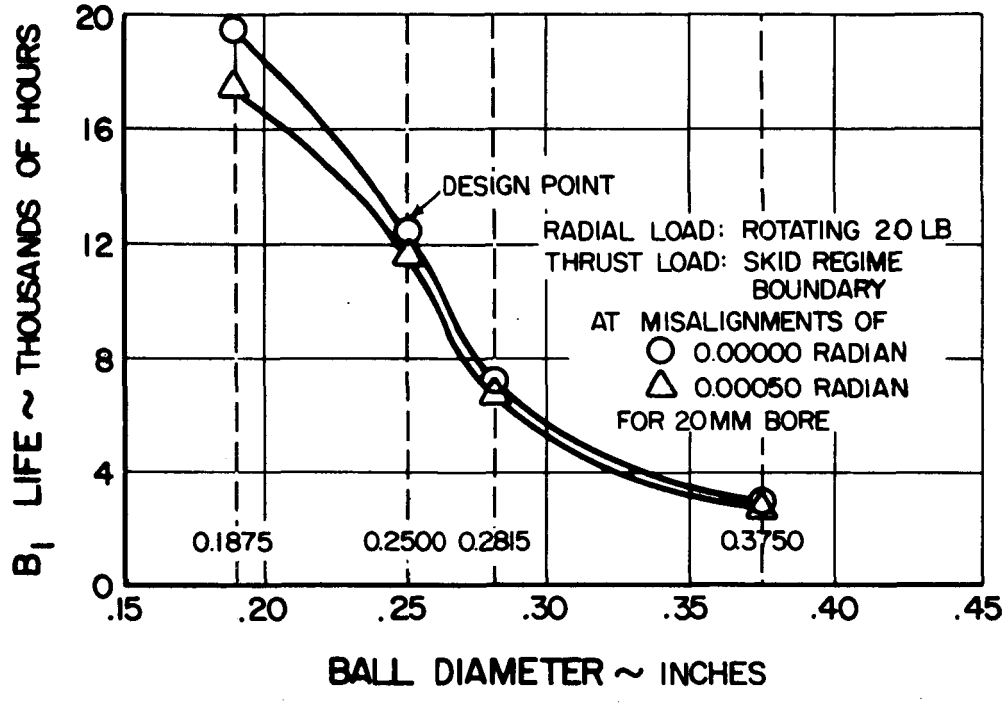

Figure 9 Bearing B_1 Life vs Ball Diameter

The effects of inner and outer race curvatures were examined and the results are presented in Figures 10 and 11. The optimum conformities are 51.75 and 51.83 per cent for the inner and outer races, respectively. (Conformity is defined as the ratio of the radius of curvature of the race to the ball diameter.) Fifty-two per cent conformity is conventional for high speed bearings and this value was selected for the turbine-compressor bearings. As indicated in Figures 10 and 11, the selected conformities do not appreciably compromise the bearing life.

The examination of the effects of mounted contact angle on bearing life is presented in Figure 12. The optimum contact angle is 16 degrees. The variation in contact angle with manufacturing tolerances and the effect of this variation on bearing life are also indicated in Figure 12.

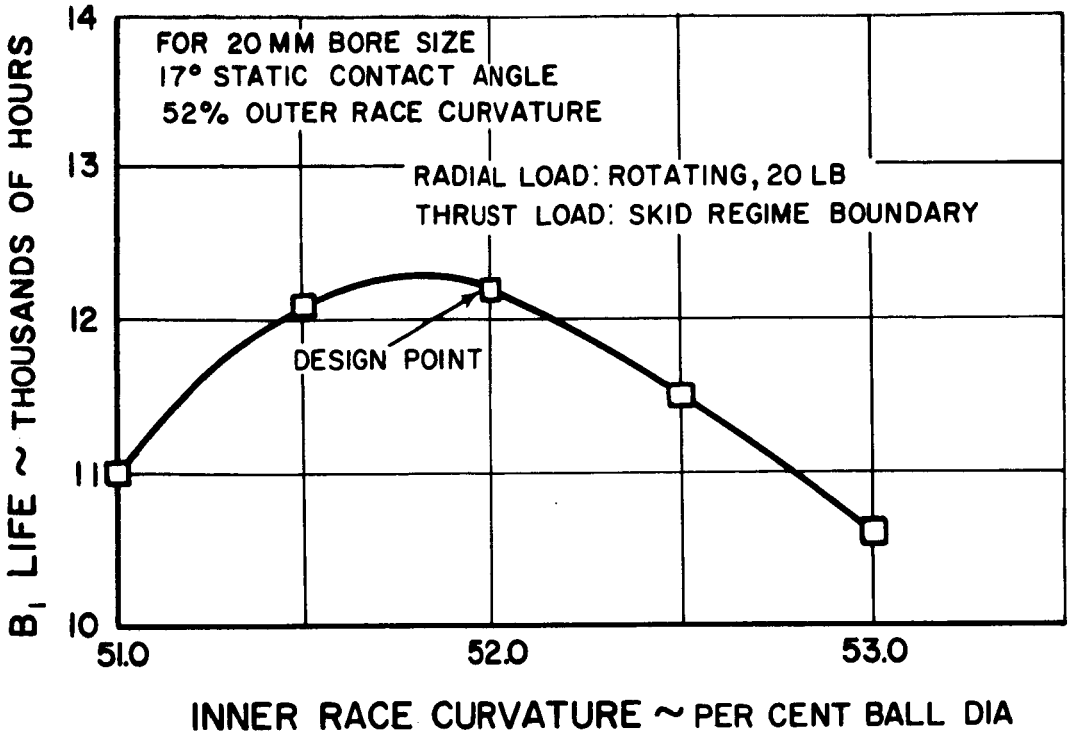

Figure 10 Bearing B_1 Life vs Inner Race Curvature

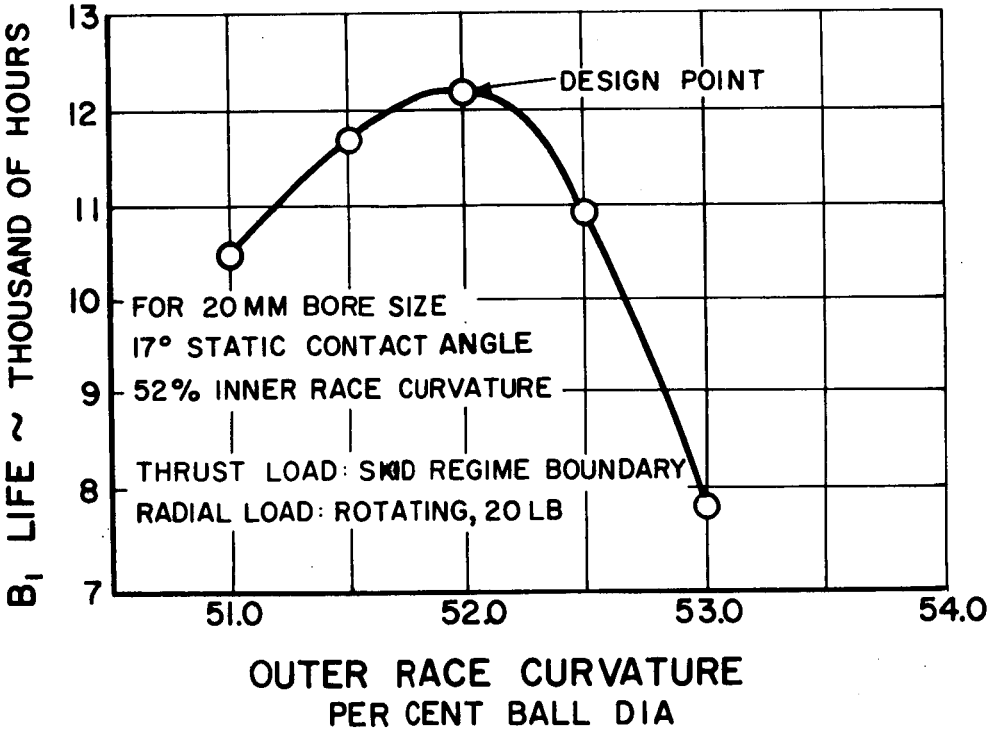

Figure 11 Bearing B_1 Life vs Outer Race Curvature

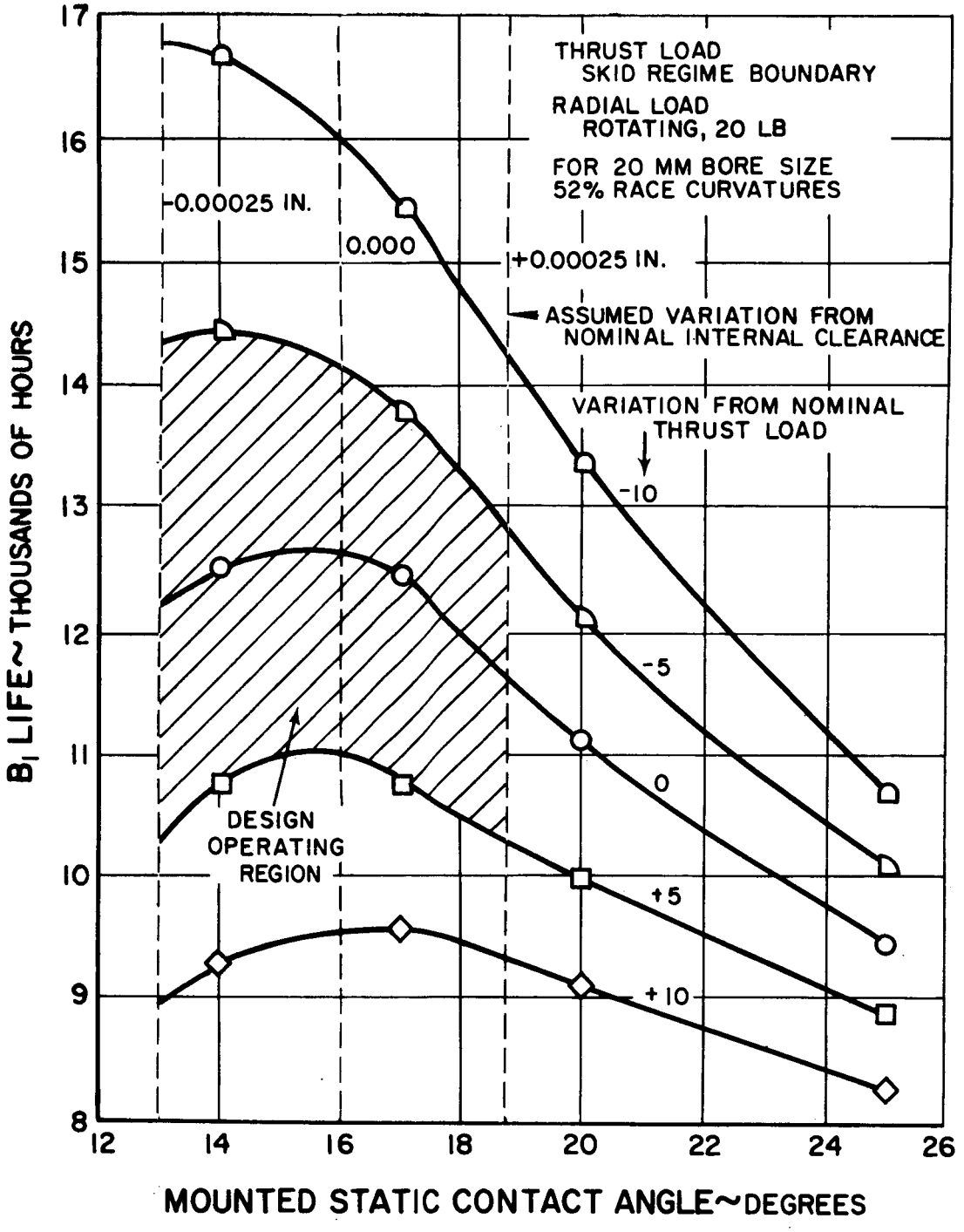

Figure 12 Bearing B_1 Life vs Mounted Static Contact Angle

With rolling-element bearings in the turbine-compressor, the aerodynamic thrust on the rotor is intended to be balanced. In order to account for possible variations in conditions, a range of aerodynamic

thrust from -5 to +5 pounds is considered which produces a total variation of approximately 25 per cent in bearing life.

All of the bearing life calculations were performed with a 20-pound radial load which is the maximum unbalance load anticipated at the end of 10,000 hours of operation. If the radial load is varied the resulting bearing life is presented in Figure 13. With no radial load imposed, the bearing life is improved about 21 per cent.

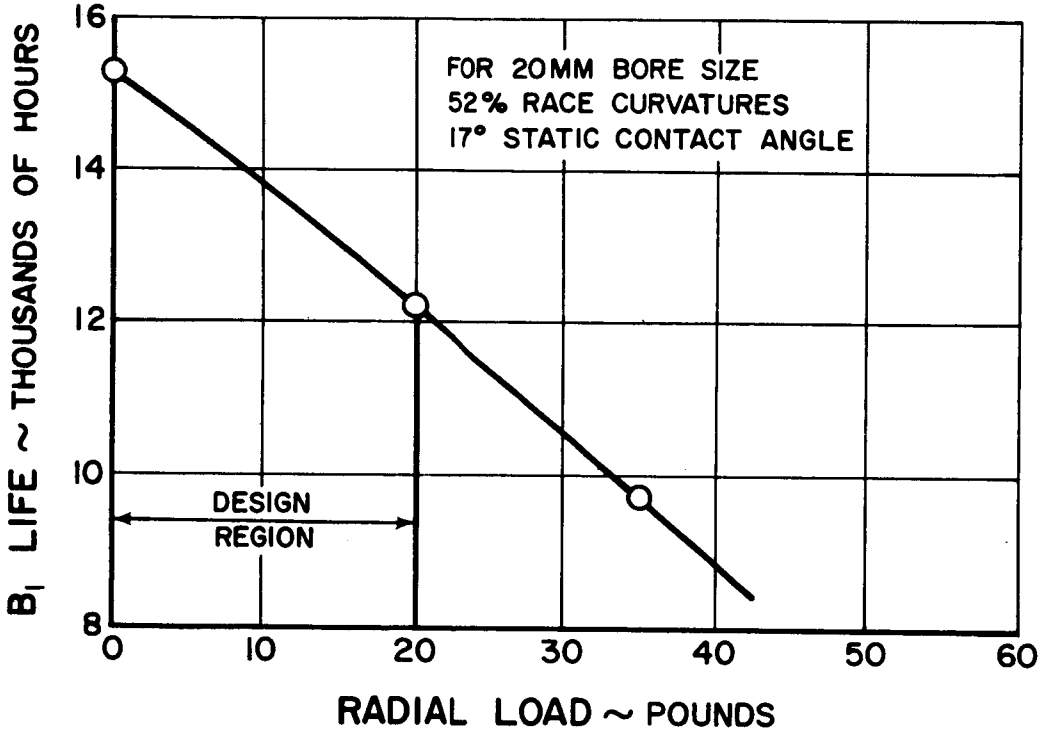

Figure 13 Bearing B_1 Life vs Radial Load

The bearing performance characteristics presented in Figures 7 through 13 are calculated at the design condition of 50,000 rpm in a gravity-free environment. These bearings will also be expected to operate with the turbine-compressor on the ground for development testing. If the shaft were horizontal in such a test, the net effect would be an increase in radial load of about 6 pounds on each bearing. An approximate indication of the associated reduction in life can be determined from Figure 8. With a 26-pound radial load, the life of the selected bearing is reduced to 11,000 hours. If the development testing were conducted in the vertical position with the compressor up, the thrust load on the rear bearing would increase by the weight of the rotor - approximately 12 pounds. The resulting B_1 life of the rear bearing is 9,500 hours, which should be satisfactory for development testing.

Since the bearing design objective was to provide maximum fatigue life consistent with low power consumption and the absence of skidding, the choice of bearing materials was carefully reviewed. Traditionally SAE 52100 steel has been the standard bearing material. Developments such as vacuum melting of SAE 52100 have considerably improved bearing fatigue life. Current aircraft turbine engines require better properties than SAE 52100 offers and considerable experience has been accumulated with better bearing materials. Consumable electrode vacuum melted M-50 tool steel has demonstrated superior fatigue life and is currently being specified for many of these high performance applications. Because of this favorable experience M-50 tool steel is specified for the turbine-compressor bearings.

The bearing life estimates include modifications to the usual AFBMA calculations based on experience in high speed application. These modifications account for the detrimental effect of centrifugal force on the balls and the advantageous effects of increased resistance to fatigue and narrower distribution of failure lives which is characteristic of the vacuum melted M-50 steel bearings. The estimated B_1 life at nominal design conditions is 12,600 hours.

Experience has shown that for high-speed long-life applications such as the Brayton cycle, the ball retainer designs must be of one-piece fully-machined construction to achieve high strength and fine balance. An inner race riding retainer is selected because of the extensive experience with this configuration, the better bearing tolerance for short interruptions of oil flow, and the ability of the inner race oil cooling to remove the heat generated in the retainer-race bearing

area. Since a one-piece retainer is selected, the only bearing configurations that can be used are the counterbore type or the split inner ring type. The risk in the split inner ring configuration is that the ball-race contact ellipse may extend to the chamfer at the split on the inner race. If this were to occur the stresses in the contact zone would be significantly increased and the bearing life would be reduced accordingly. The variation in mounted contact angle resulting from allowable internal tolerances is shown in Figure 12. While the calculations indicate that the ball would not ride on the chamfer at the split, some transient radial load might produce such a condition. Therefore, the counterbore configuration, which employs a solid inner ring, was selected.

In summary, the bearing selected and recommended for the turbine-compressor is a 20 mm bore extra light series ball bearing constructed of M-50 steel with a one-piece cage. The selected bearing design requirements are as follows:

Bearing Type	Angular contact ball bearing with counterbore outer race
Operating Conditions	Thrust load: 30 pounds Rotating unbalance radial load: 20 pounds maximum at 50,000 rpm
Oiling System	Mist lubrication Axial cooling slots on bore of inner ring
Heat Generation	125 watts/bearing
Bearing Size	20 mm bore diameter 44 mm outer diameter 12 mm wide
Internal Geometry	11 balls of 0.2500 inch diameter 1.288 inch pitch diameter (slightly larger than standard extra light dimensions) 16° nominal mounted contact angle at operating fits and clearances 52 per cent inner and outer race conformity 10 per cent shoulder height on the loaded half of outer race 20 per cent inner race shoulder height

V. TURBOALTERNATOR DESIGN

The basic turboalternator design task under this program is to provide a rolling-element bearing system design that can be used as an alternate to the gas bearings presently being developed under Contract NAS3-6013. The overall objectives of the rolling-element bearing design for the turboalternator are identical to those of the similar turbine-compressor design task discussed in Section IV.

A. Mechanical Arrangement

The mechanical arrangement of the turboalternator, shown in Figure 14 with rolling-element bearings, is essentially the same as the arrangement with gas bearings. Radial rotor support is provided on each side of the alternator and the turbine is overhung. A roller bearing is located between the turbine and alternator and a ball bearing is placed at the free end of the alternator to support both radial and thrust loads. Since the rotor speed is only 12,000 rpm, bearing skidding is not a problem. One seal is employed between the roller bearing and the turbine. No seal is required on the free end of the alternator. As a result some oil may migrate into the alternator cavity, but argon from the exit of the separator flows through the alternator cavity to prevent excessive oil accumulation in this cavity. The gas pressure in the cavity is essentially the same as in the bearing compartment, which is a little higher than compressor inlet pressure. With this low pressure the alternator windage is kept to a minimum.

The turbomachinery requires that the oil be separated from the argon which leaks through the seals before this argon is returned to the main cycle. A rotary separator is located on the free end of the alternator to separate oil droplets from the argon. This is a convenient location for the separator. Operation at 12,000 rpm provides lower losses than operation at turbine-compressor speed. Also the thermal environment of the separator is advantageous at this location.

B. Critical Speed Analysis

The critical speeds of the preliminary turboalternator arrangement shown in Figure 14 have been analyzed assuming essentially stiff bearing

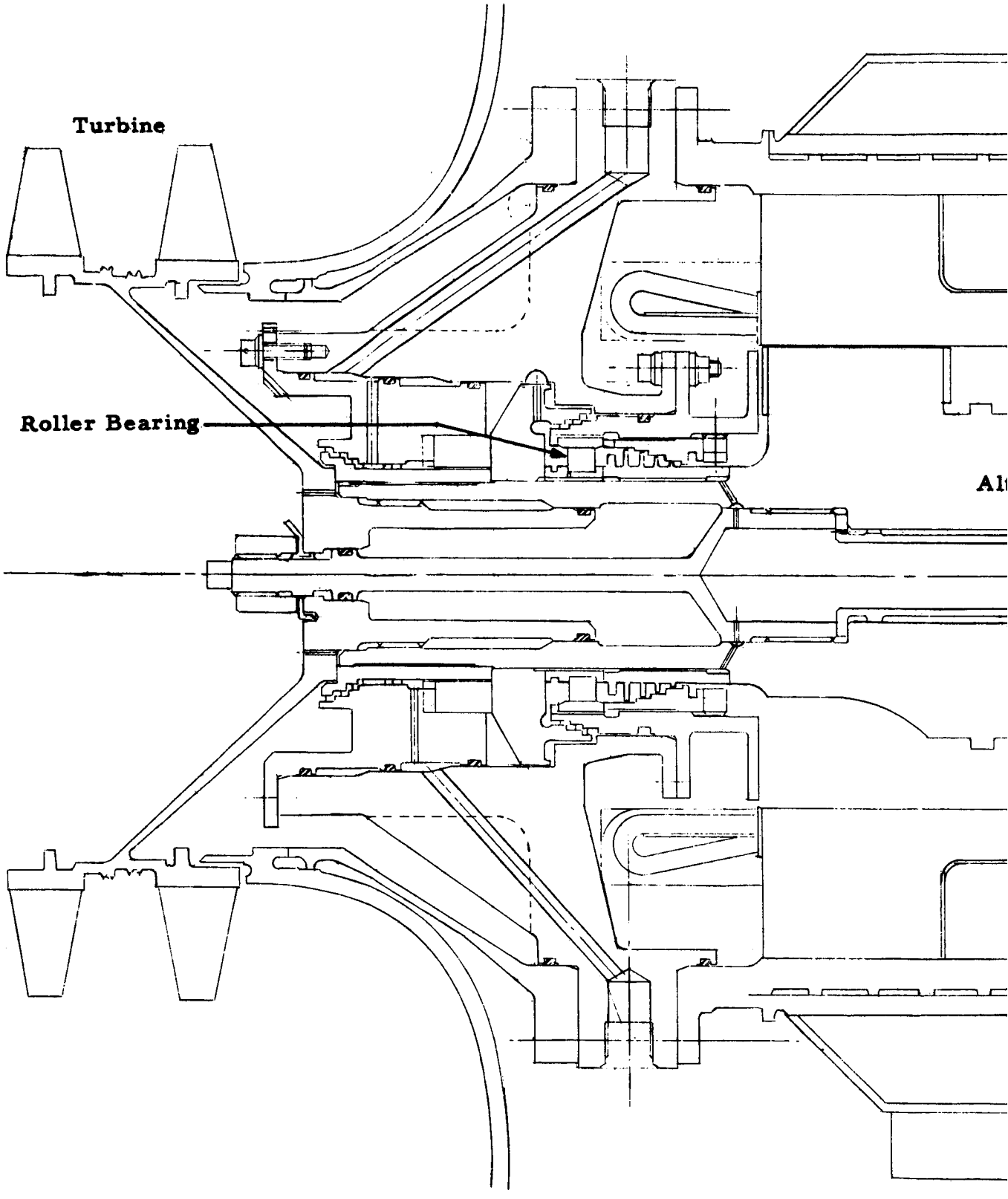

Figure 14 Brayton-Cycle Turboalternator. Preliminary Rolling-Contact Bearing Arrangement

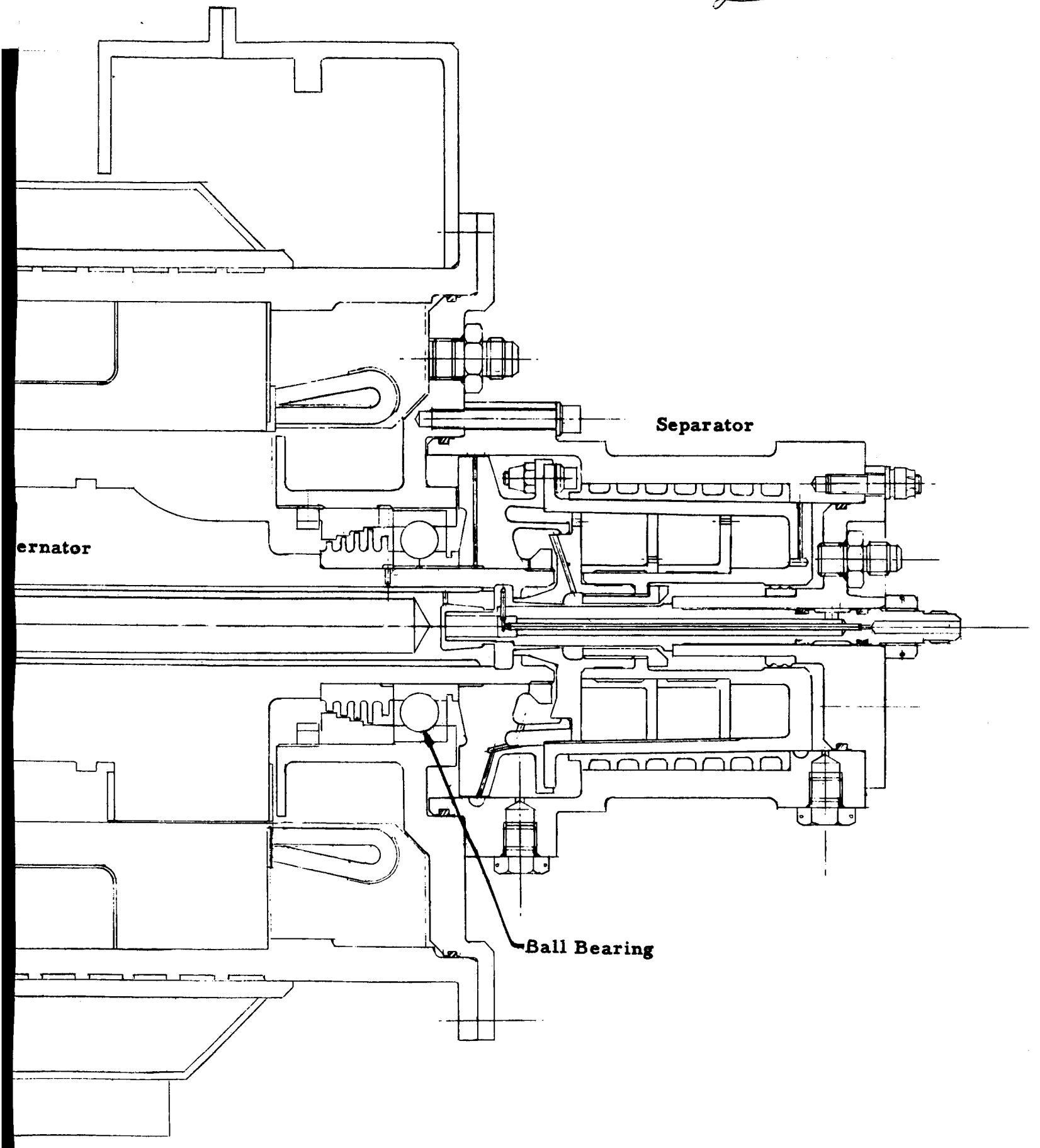
Separator
ernator
Ball Bearing

supports. The resulting first, second, and third resonant modes are presented in Figure 15 as a function of effective bearing spring rates. The effective bearing stiffness is in the range of 500,000 to 1,500,000 pounds/inch. The first critical speed is a rigid-body conical mode which occurs at over twice the design speed in the range of interest. The second critical speed is a rigid-body translation mode and the third is the bent-shaft or free-free mode. Evidently, at the effective bearing spring rate currently planned, all of the critical speeds are well above the operating speed.

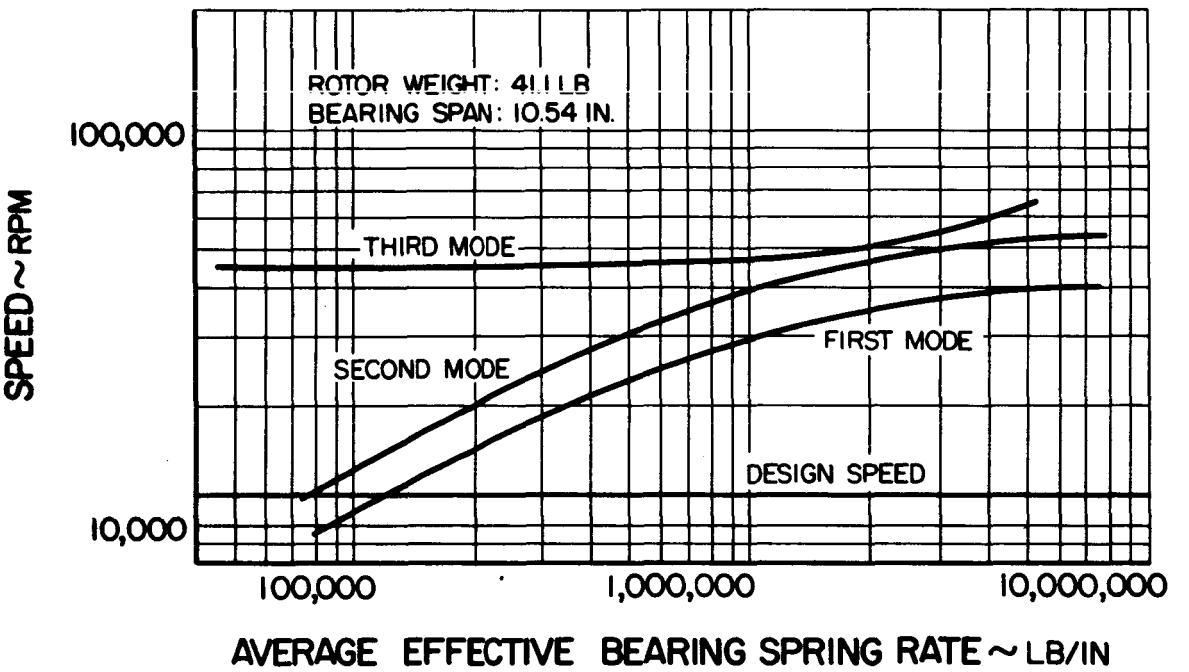

Figure 15 Preliminary Turboalternator Critical Speeds

VI. LUBRICANT EVALUATION

A. Lubricant Selection

The lubrication system shown schematically in Figure 2 and described in Section III is a closed single-charge system with sufficient inventory to last the projected mission life of 10,000 hours. The lubricant is used to cool and lubricate the bearings and seals in both the turbine-compressor and turboalternator. Hence, it is subjected to a range of temperatures from 100 to 400°F as it circulates through the system. In order to conserve the oil and argon inventories and to prevent contamination of the cycle argon, the argon that leaks past the seals into the bearing compartment must be separated from the oil and returned to the main cycle. Considering these system conditions and requirements, a list of desirable lubricant properties is as follows:

1) The lubricant must have favorable long-time lubricating characteristics for high-speed bearings and seals.

2) The lubricant must be thermally stable.

3) Any decomposition that takes place should not yield products harmful to either the lubricant or the powerplant.

4) The lubricant should have good heat transfer characteristics.

5) The lubricant must be chemically compatible with the various structural materials used throughout the system.

6) The vapor pressure and solubility of the oil in argon and argon in oil must be favorable. Heat transfer, lubricating, scavenging and separation characteristics could be adversely affected.

7) The viscosity characteristics must be compatible with the operating temperatures.

Three candidate lubricants are being considered for this application, 1) five-ring polyphenyl ether (PWA-524), 2) four-ring polyphenyl ether (Monsanto MCS-333), and 3) super-refined mineral oil (MLO-7277). Factors considered in comparing the three lubricants during this report period are shown in Table 1.

TABLE 1

Lubricant Comparison

Property	Lubricant			Remarks
	Super-Refined Mineral Oil	Four-Ring Polyphenyl Ether	Five-Ring Polyphenyl Ether	
	A	B	C	
density lb/ft^3 at 350°F	49	66	68	
vapor pressure mm Hg at 350°F	0.38	0.11	0.03	
specific heat btu/lb/°F at 350°F	0.59	0.47	0.57	
thermal conductivity btu/ft/hr/°F at 350°F	0.0688	0.0686	0.0684	
viscosity Cs at 350°F	2.3	1.9	2.8	
ASTM pour point, °F	-30	10	40	
corrosiveness in air environment, method: FS791-5380 test duration: 48 hrs. at temperature of:	347°F	500°F	600°F	tests of an inhibited 5-ring polyphenyl yielded following results at 600°F
wt. change, mg/cm^2				
magnesium	+0.07	-0.06	+0.25	+0.02
aluminum	+0.07	+0.01	+0.01	+0.01
steel	+0.08	+0.03	+0.05	+0.04
copper	+0.02	-0.01	-0.95	+0.29
silver	+0.01	-0.05	+0.32	-0.12
thermal decomposition rate in inert environment at 400°F; per cent/hour	1.0×10^{-4}	6.4×10^{-10}	-	four and five-ring polyphenyl ethers are believed to have similar decomposition rates

Low temperature decomposition characteristics of the candidate oils were examined to determine if each lubricant is adequate for the mission life of 10,000 hours. At 400°F 1 per cent of the mineral oil will decompose in 10,000 hours. The4-ring polyphenyl ether has a decomposition rate which is over 5 orders of magnitude smaller. While no decomposition data is available for the 5-ring polyphenyl ether, it is expected to be similar to the 4-ring oil. Low-temperature decomposition of the 4-ring polyphenyl ether begins with the breaking of the carbon-oxygen bond and the formation of heavier and lighter ethers. At high temperatures benzene, phenol, diphenyl ether and some volatiles would form. It is believed that the products of decomposition would not accumulate in sufficient quantity to affect the physical properties of the lubricant for the duration of the mission. The decomposition rate of the mineral oil and the 4-ring polyphenyl ether are presented in Figure 16.

The chemical compatibility of the candidate oils was compared and the results are summarized in Table 1. The mineral oil at 350°F is about as corrosive as the 4-ring polyphenyl ether at 500°F. The 5-ring polyphenyl ether attacks copper to some extent at 600°F. In general, the candidate oils exhibit reasonable chemical compatibility for the intended application.

The heat transfer properties of the candidate oils were examined and the differences would not significantly affect the performance of the lubrication system. The density, specific heat, and thermal conductivity of the candidate oils are presented in Figures 17, 18, and 19.

The centrifugal separator upstream of the adsorber can efficiently remove oil droplets carried by the argon, but the separator will not remove oil vapor. The oil vapor must be removed in the adsorber and the amount of oil vapor in the argon will determine the size of the adsorber required. Therefore, low vapor pressure is a desirable property of the oil. The vapor pressure of the candidate oils is presented in Figure 20. The polyphenyl ethers exhibit lower vapor pressure than the mineral oil.

The oil must serve as a lubricant and must have a reasonable viscosity. The low-pressure viscosity characteristics of the three oils is presented in Figure 21. Actually, the more important property is the viscosity of the oil under the high pressures encountered in the contact between the ball and race. Unfortunately, such data are not normally directly avail-

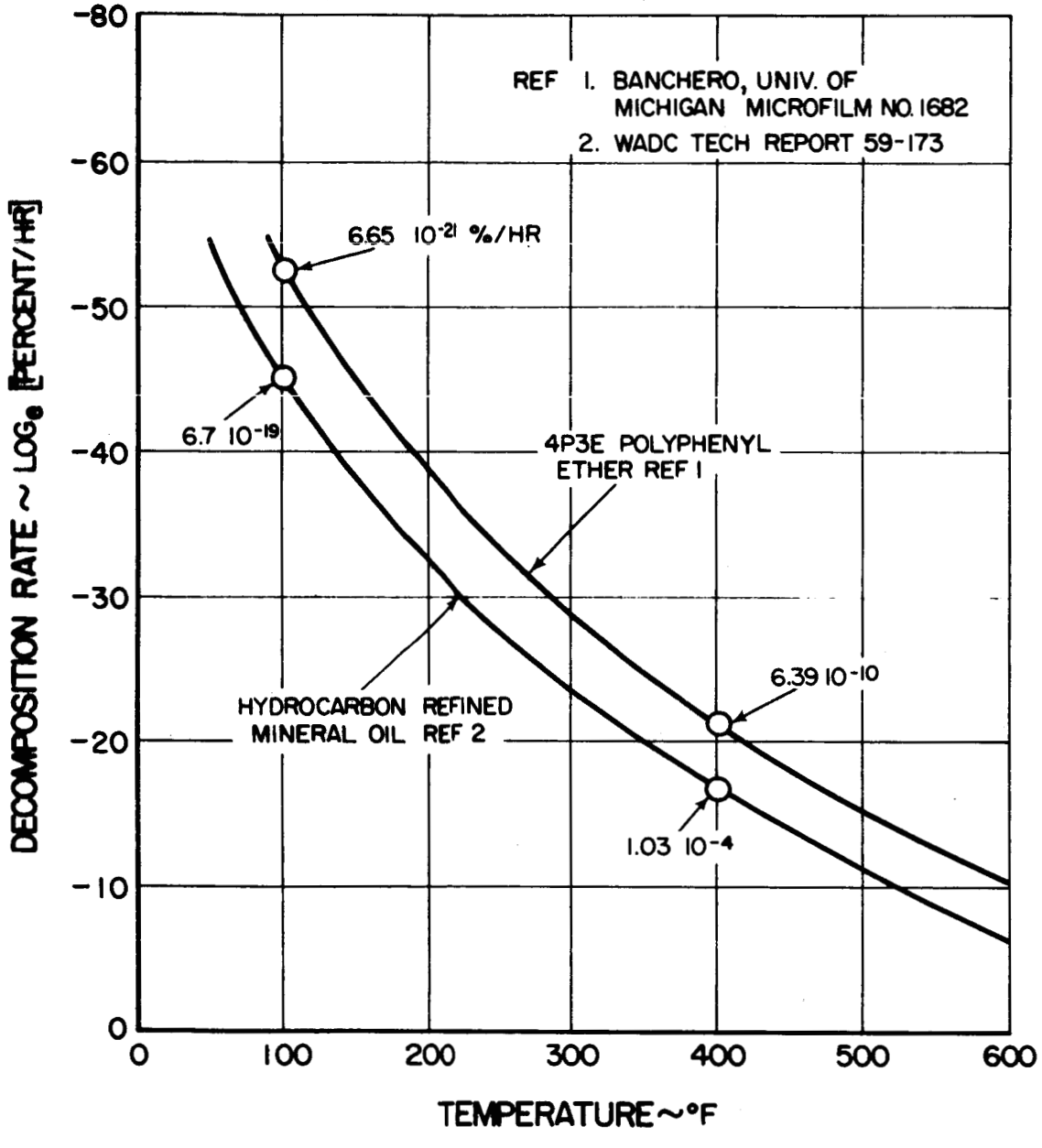

Figure 16 Thermal Decomposition Rate in Inert Environment vs Temperature

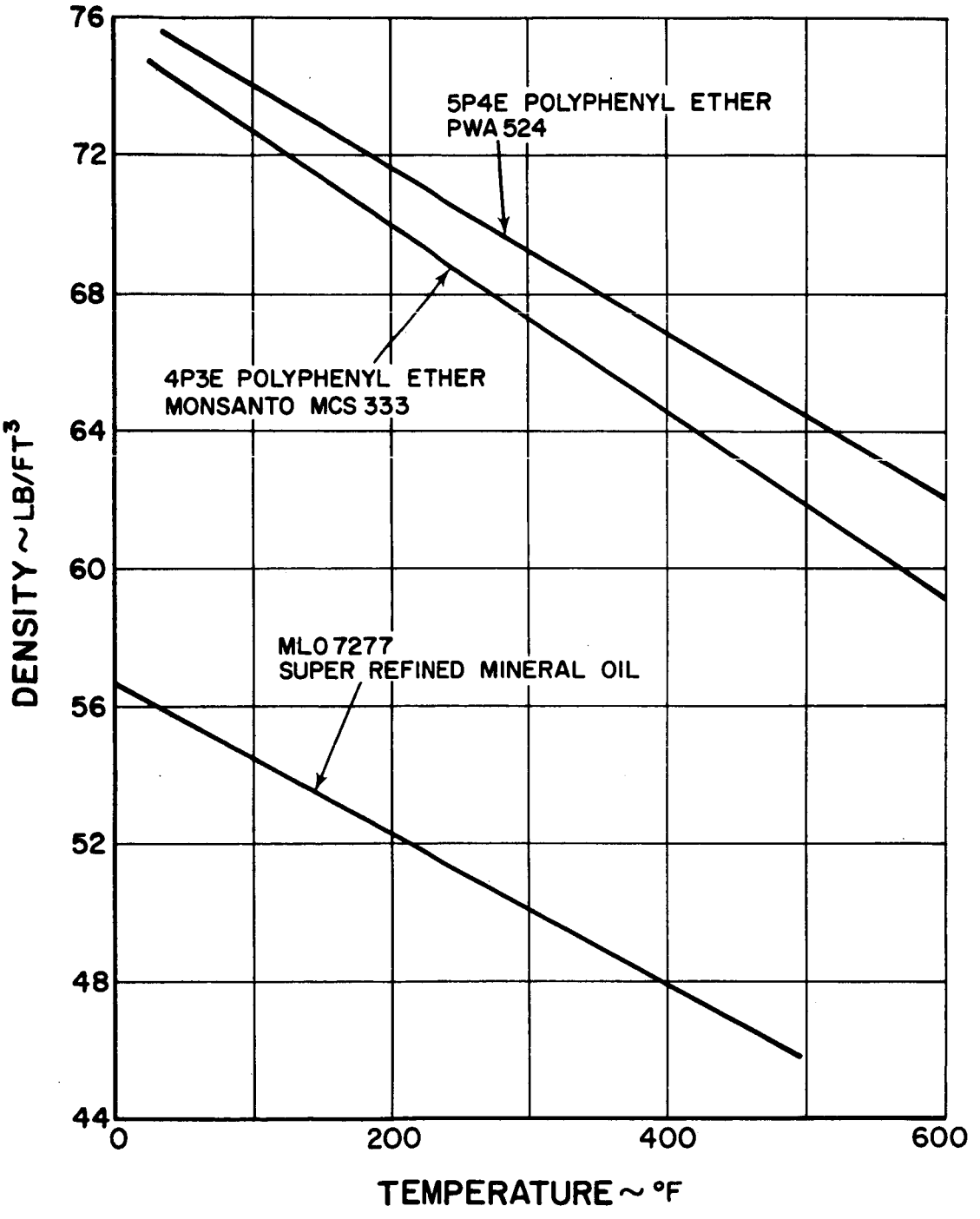

Figure 17 Density vs Temperature

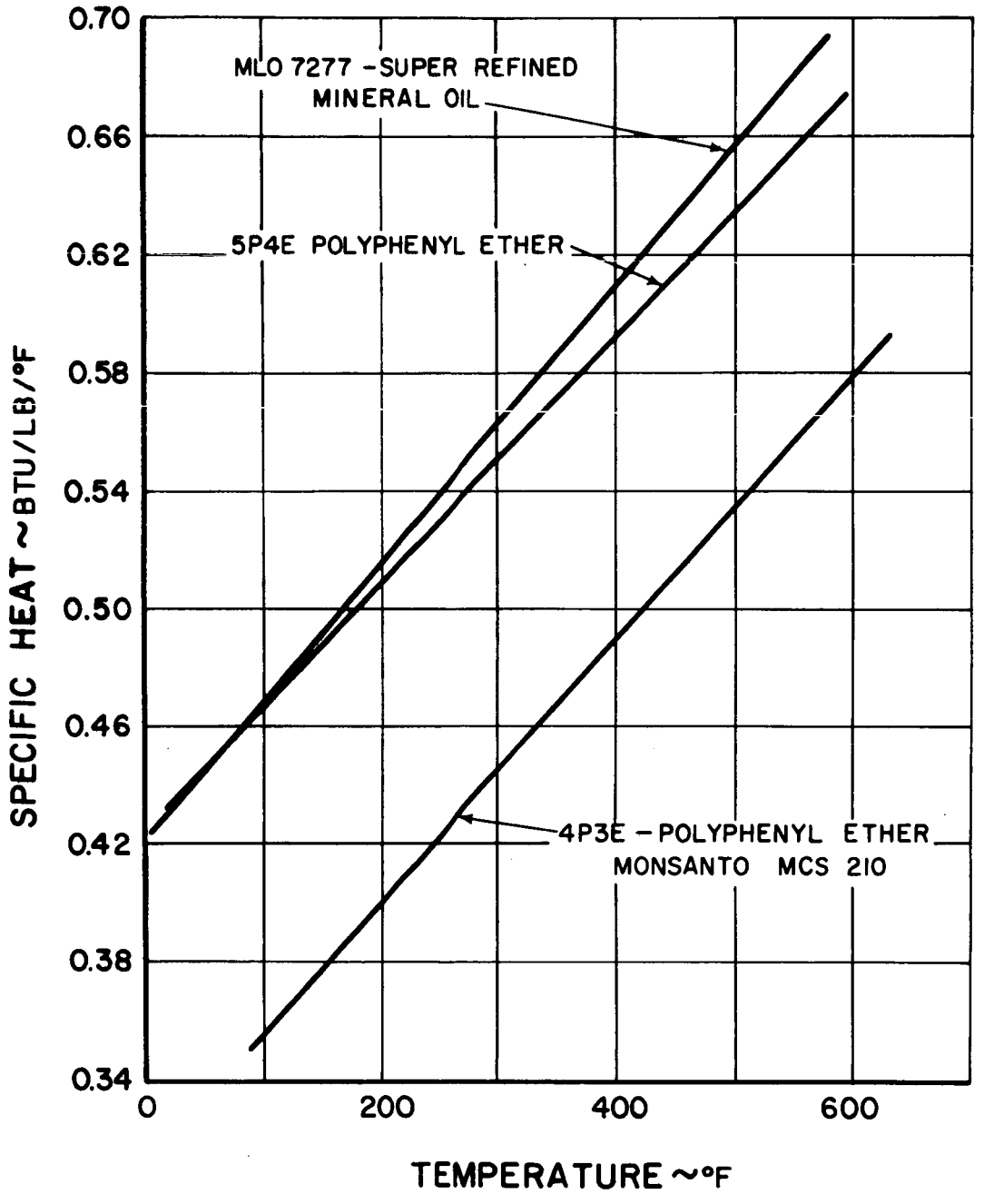

Figure 18 Specific Heat vs Temperature

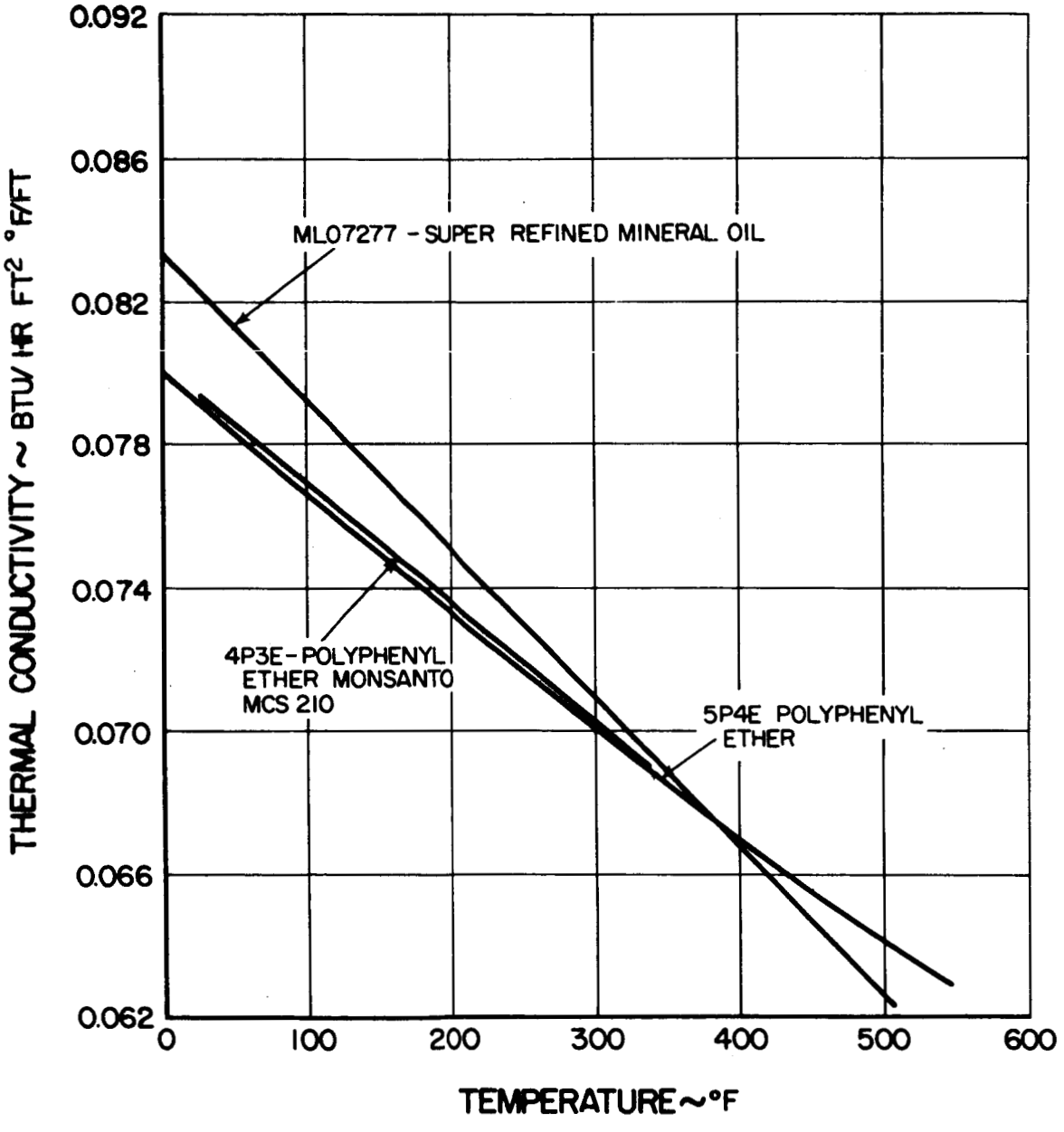

Figure 19 Thermal Conductivity vs Temperature

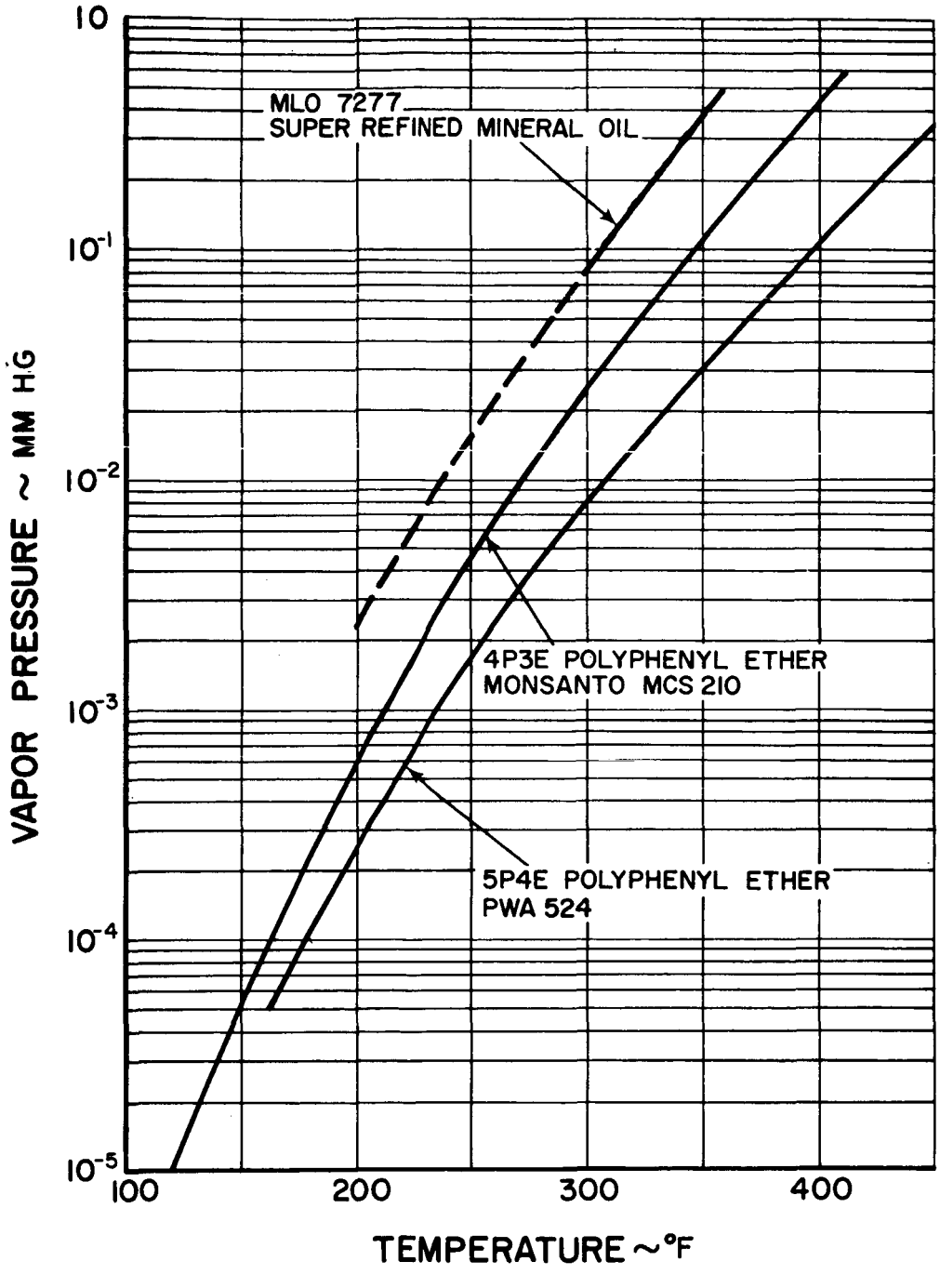

Figure 20 Vapor Pressure vs Temperature

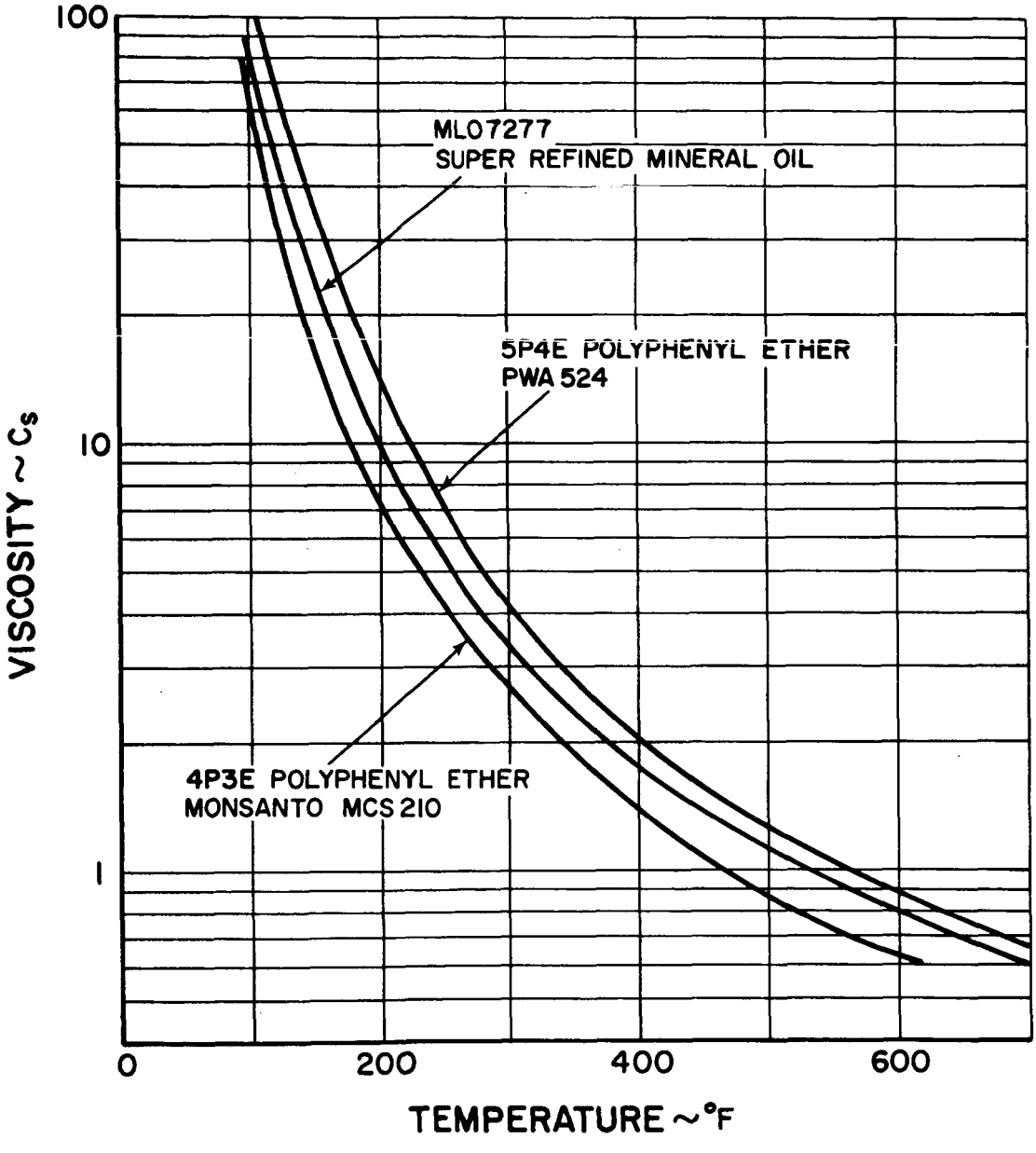

Figure 21 Viscosity vs Temperature

able and the results of indirect tests are usually required. Battelle Memorial Institute (Reference 1) has conducted rheology experiments on some oils using X-ray techniques to indicate film strength and lubrication properties. The results of tests with a highly refined mineral oil and a 5-ring polyphenyl ether are presented in Figures 22 and 23. The polyphenyl ether provides larger oil film thickness and lower pressure than the mineral oil in these tests. NASA has conducted tests of the wear characteristics of MLO 7277 mineral oil with additives, and of a 4-ring polyphenyl ether without additives in a 5-ball tester. The results of these tests have not yet been published but the preliminary indications are that the mineral oil produced better results. Pratt & Whitney Aircraft has tested a 5-ring polyphenyl ether with additives in high-speed ball bearings with excellent endurance results. Evidently, a direct comparison of the lubricating properties of the candidate oils is not possible based on the data available at this time. Therefore, one oil is not clearly superior to the others for the the Brayton-cycle application and further investigations are required.

B. Lubricant Contamination Investigation

The consequences of lubricant contamination of the Brayton-cycle working fluid were investigated. The objective of this study was to determine the maximum amount of oil contamination allowable for a 10,000-hour mission. The investigation is concerned with three basic areas.

1) Identification of the products formed by pyrolysis (thermal decomposition) of the lubricant.

2) The distribution or location where the various products of the pyrolysis will accumulate in the system.

3) The consequences to powerplant performance of oil contamination in certain locations due to the fouling of heat transfer surfaces, blockage of flow passages, and introduction of gases into the argon.

The existing data on the kinetics and the resultant products of the pyrolysis reactions are insufficient to make good predictions of the consequences of lubricant contamination of the primary cycle. Data do not extend to the high temperatures found in the cycle and data are not available for pyrolysis with low oil contamination in the argon gas, which is the pertinent condition. Some quantitative predictions have been made by extrapolating existing data and by the application of physical chemistry theory. The

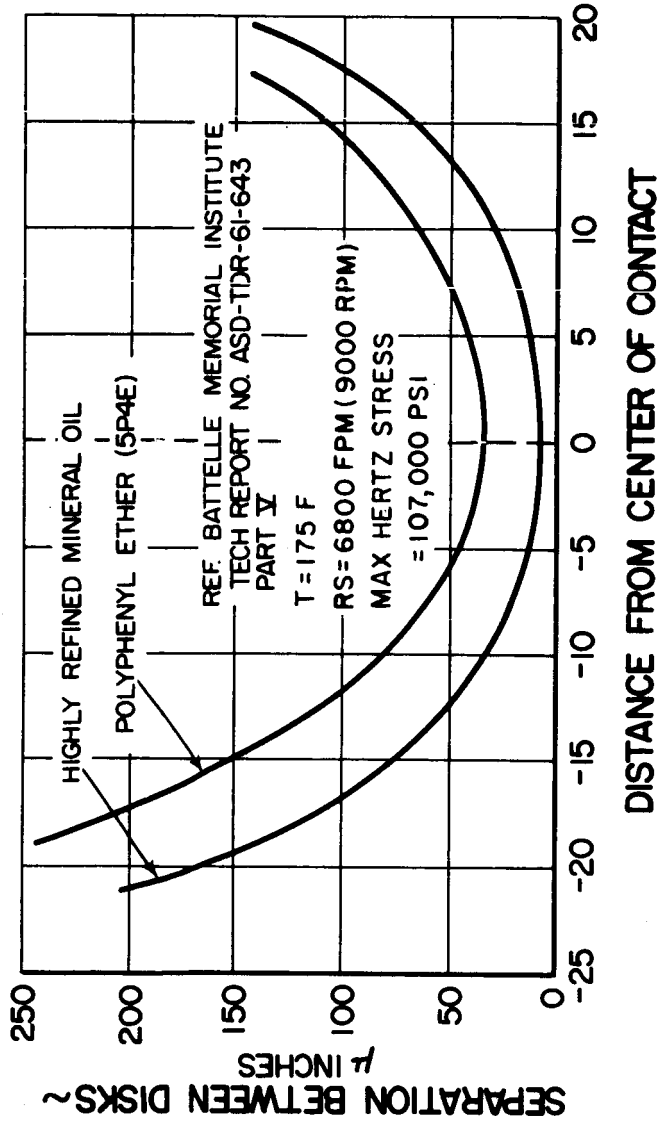

Figure 22 Circumferential Profile of Lubricated Rolling Discs

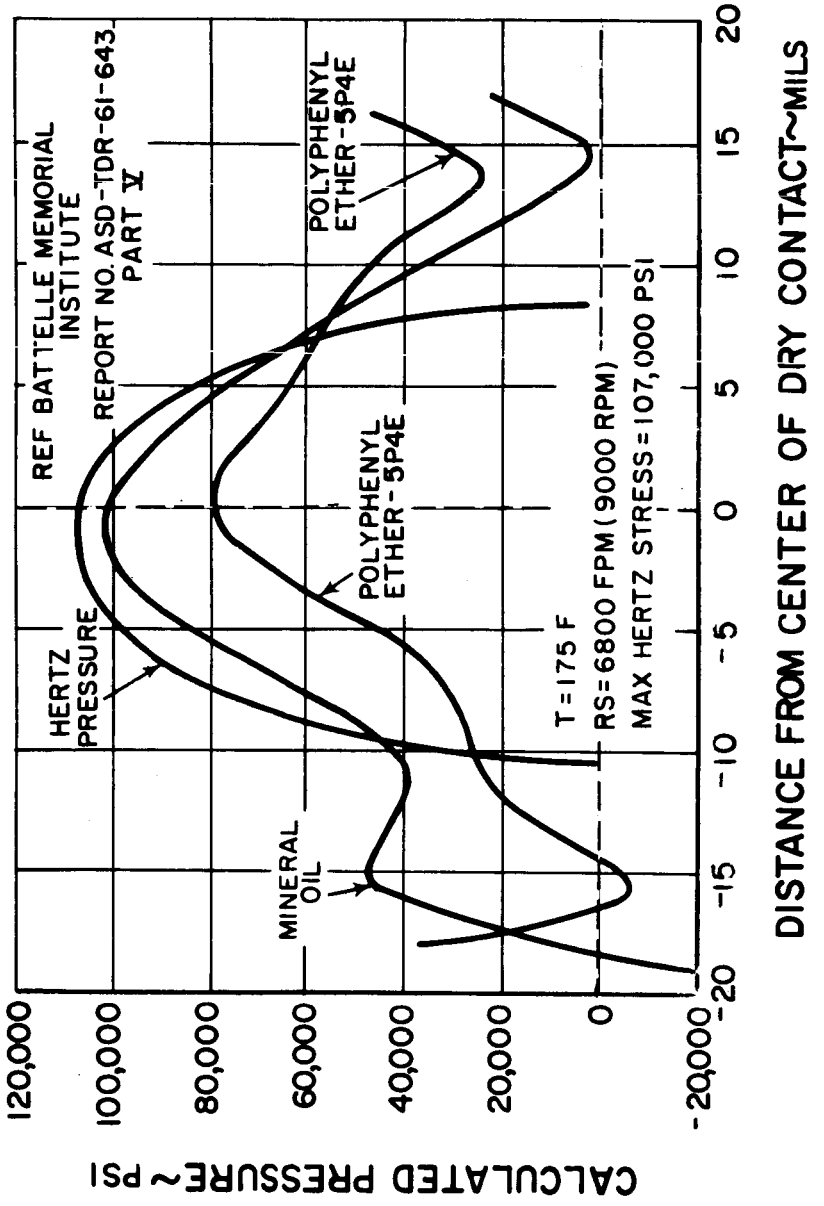

Figure 23 Pressures Calculated from Circumferential Profiles

results of these predictions indicate that aliphatic organic compounds such as MIL-L-7808C and MLO-7277 will form large quantities of gaseous products and coke (chiefly carbon, some polymer). The aromatic compounds such as the polyphenyl ether will yield tar (chiefly polymer, some carbon) and a small quantity of gases upon pyrolysis in the Brayton-cycle loop.

The anticipated distribution of the oil pyrolysis products is as follows: Solid products are built up in the hotter areas, such as the heater where the high temperature exists and therefore where high pyrolysis reaction rates will occur. Gaseous products formed may be adsorbed in the molecular sieve (adsorber in the oil separation system). Of course, these products must first leak through the seals before passing through the adsorber. Gaseous hydrogen will accumulate in the fluid unless special precautions are introduced to prevent such an accumulation. For example, a palladium section located in the Brayton-cycle loop would permit hydrogen to leak from the loop while retaining the argon. If the oil is a polyphenyl ether, there is a possibility that some low-volatility liquid products may condense in the cooler parts of the system.

Quantitative assessment of the oil contamination is limited to extrapolations and approximations due to the lack of definitive data on the particular reactions involved. Approximate analysis indicates that the uniform deposition of coke or tar in the heater will reduce system performance due to the increase in flow resistance. If the Brayton-cycle efficiency were reduced approximately 1-1/2 per cent which corresponds to an increase in $\Delta P/P$ of approximately 0.02 and assuming a relatively uniform deposit of material, the system would be able to adsorb something over 5 pounds of oil in the course of the mission. The effect of such deposits on heat transfer coefficients is relatively small because the thermal resistance of the gas film is fairly high. The release of hydrogen will affect the cycle performance. If the gas pressure is allowed to build up and if a constant temperature source is employed, the power output of the system would increase with small amounts of hydrogen added to the argon. Actually the heat source may be limited in capacity and if a constant heat input were employed, the cycle output would be reduced with small amounts of hydrogen added to the argon. Approximately 0.002 to 0.003 pound of hydrogen would produce a loss in power of 10 per cent. Since between 5 and 15 per cent of the oil molecular weight is hydrogen, this level of hydrogen release would correspond to 0.02 to 0.06 pound of oil contamination in the

course of the mission. Actually, hydrogen can be selectively released from the system so that these very small quantities of oil contamination do not have to be the limiting criteria.

Appendix 1 describes in further detail the investigation of the effects of oil contamination in the basic cycle.

VII. ADSORBER INVESTIGATION

In Section VI the effects of oil contamination in the Brayton-cycle argon working fluid are discussed. One conclusion of this investigation is that the oil which enters the primary cycle fluid must be restricted to very small quantities in the course of the 10,000-hour mission. A combination of labyrinth and face seals separates the lubricant in the bearing compartments from the argon in the main cycle. However, argon will leak into the bearing compartment and this gas must be returned to the primary cycle free of oil or oil vapor. As shown in the schematic diagram, Figure 2, the oil droplets are removed from the argon in the centrifugal separator. In order to reduce the quantity of oil vapor carried with the argon, the mixture is cooled to about 100°F in the separator. The argon gas containing oil vapor then passes through a molecular sieve or adsorber which adsorbs the oil vapor while permitting the argon to pass through to the primary cycle at the compressor inlet.

In order to evaluate adsorber materials and to provide data to produce an efficient adsorber design, an adsorber test rig has been designed and constructed. A schematic diagram and a photograph of this test apparatus are presented in Figures 24 and 25. Metered argon is injected into a heated oil bath vaporizor which produces an argon-oil mixture containing both soluble and entrained oil constituents. The oil-gas mixture is cooled after it leaves the vaporizer to a temperature corresponding to the entrance to the adsorber in the flight configuration. This cooling produces an aerosol which is carried to a separator assembly. The separator utilizes gravity to simulate the centrifugal separator in the turboalternator. After leaving the separator the gas-oil mixture passes through the adsorber and the exhaust of the adsorber is piped to a chromatograph which is shown in Figure 26.

The chromatograph measures any residual oil in the argon. A bypass around the adsorber is included to permit analysis of the oil-argon mixture entering the adsorber. A wet-test meter is employed to precisely measure the argon flow rate in the test rig. Temperature and pressure measurements are provided as indicated in the schematic drawing of the rig, Figure 24.

Initial calibration and checkout of the test rig is being conducted using available polyphenyl ether in the vaporizer and Linde 4a molecular sieve

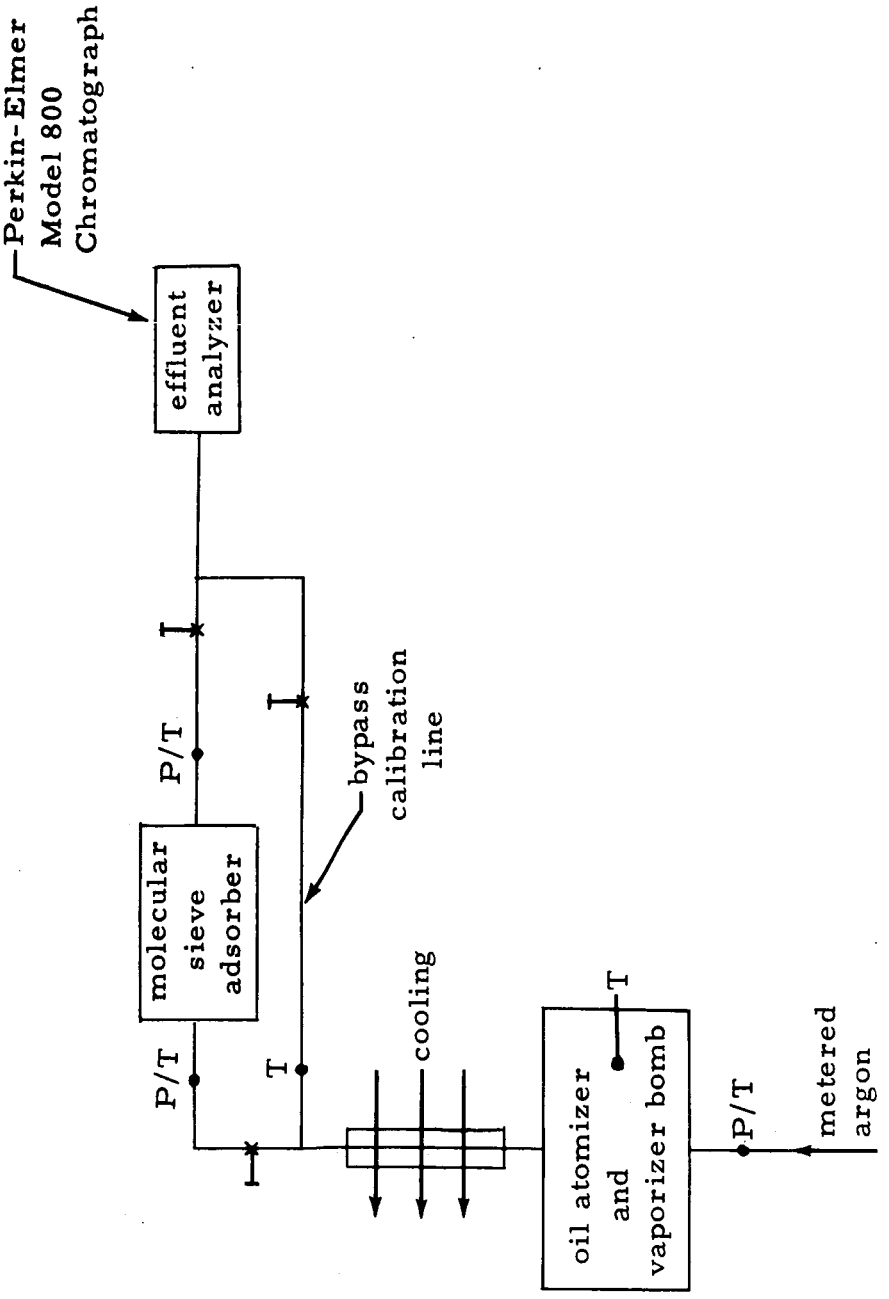

Figure 24 Schematic Diagram of Adsorbate Evaluation Apparatus

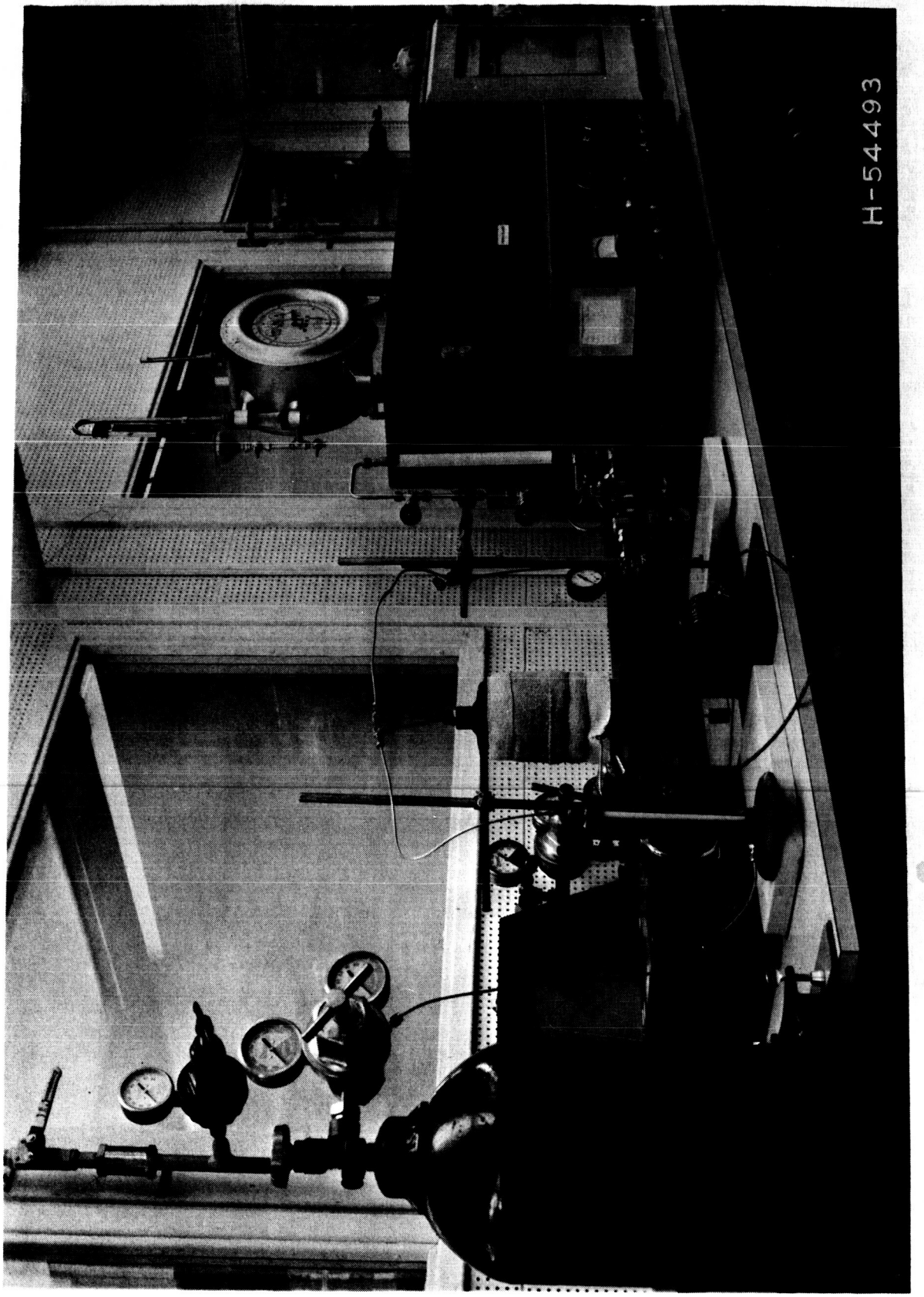

Figure 25 Test Apparatus for Adsorbate Evaluation

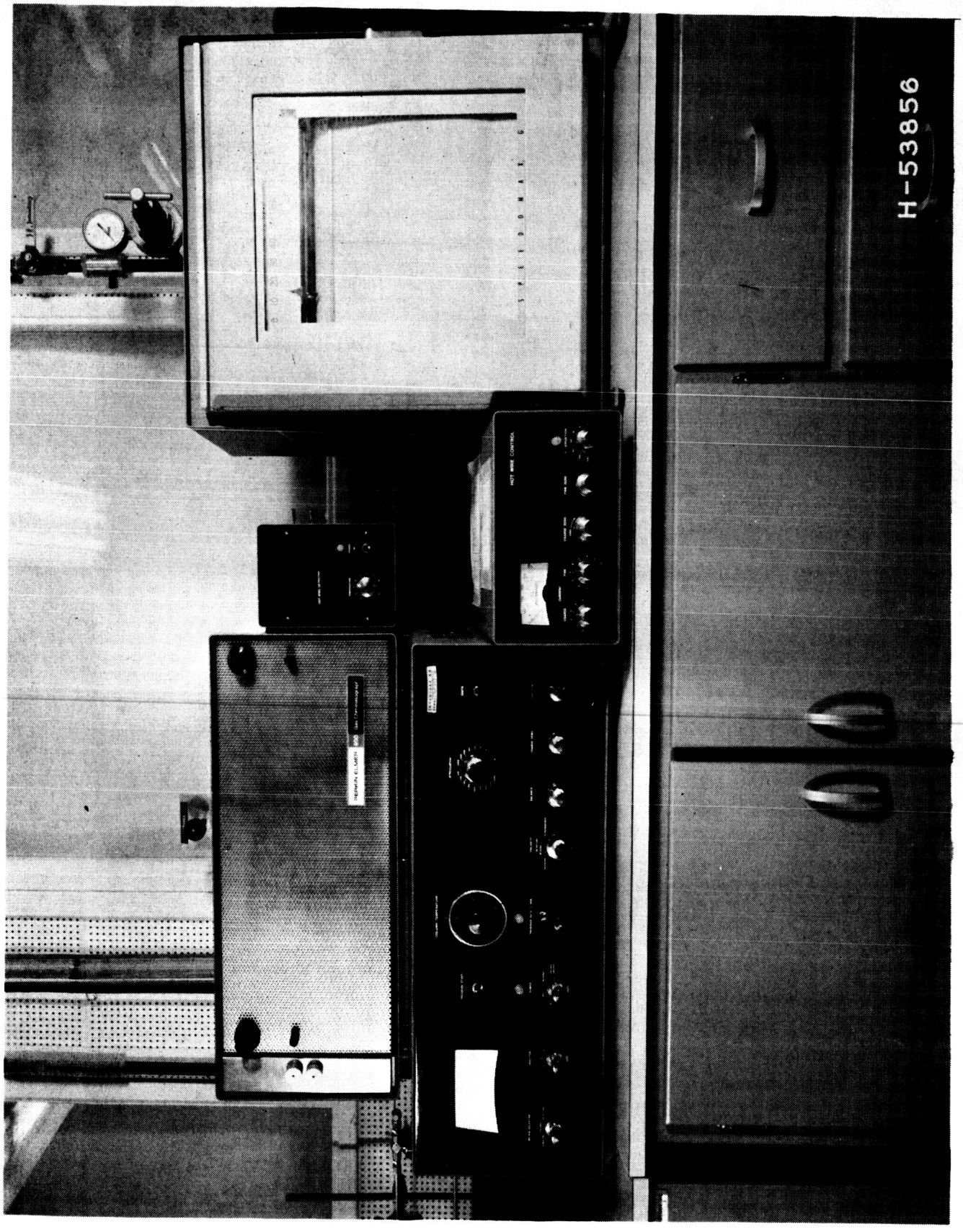

Figure 26 Perkin-Elmer Model 800 Chromatograph

material in the adsorber section. Additional molecular sieve materials including Linde 13x are being procured. A Pyrex tube has been utilized to contain the adsorber material. With this arrangement, channeling through the adsorber bed was observed with the column orientated horizontally. The orientation of the column was changed to vertical and channeling was no longer observed. Future adsorber column designs will require baffling or other geometric control of the adsorber material to preclude channeling under weightless conditions. Initial tests have also been concerned with developing the instrumentation techniques to determine oil content in the argon gas leaving the adsorber.

In order to more fully evaluate the properties of the adsorber materials of interest, plans include investigation of the particle size and relation of surface area to volume of the adsorber material, using equipment shown in Figures 27 and 28.

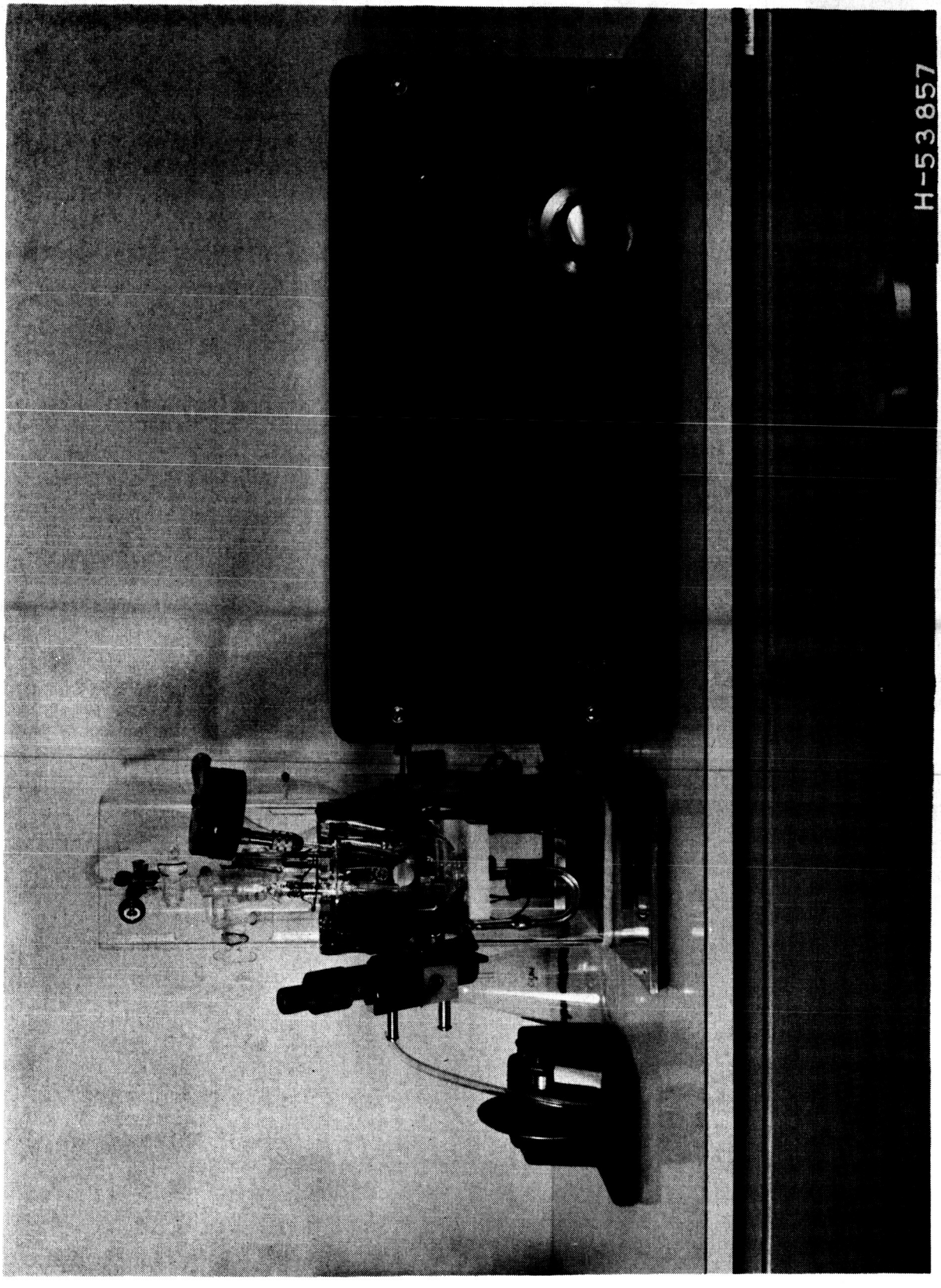

Figure 27 Coulter Counter for Determination of Adsorbate Particle Size

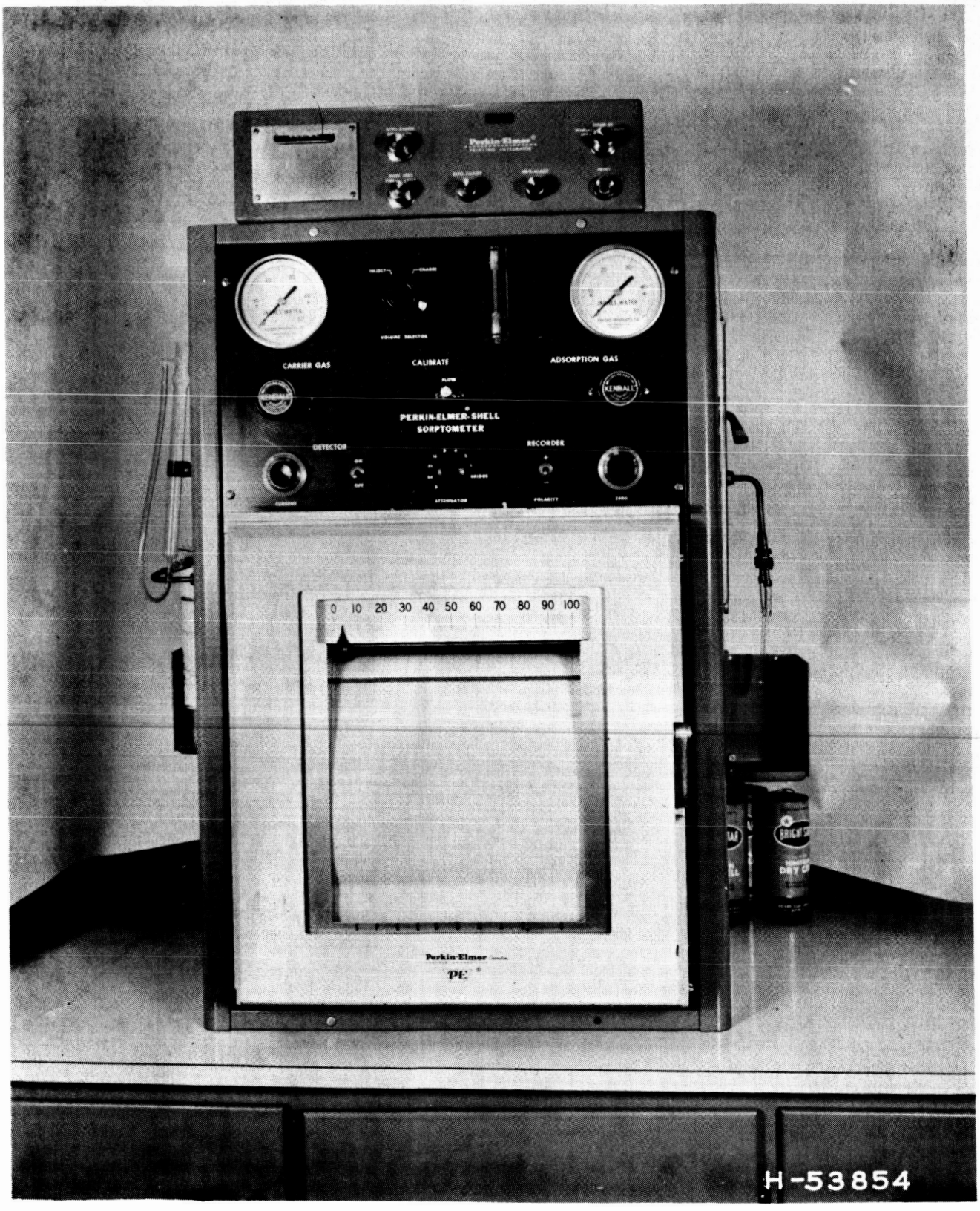

Figure 23 Perkin-Elmer Sorptometer for Measurement of Total Surface Area of Adsorbate Bed

APPENDIX 1

Brayton-Cycle Performance Effects of Oil Contamination

APPENDIX 1

Brayton-Cycle Performance Effects of Oil Contamination

A. Introduction

1. Brayton-Cycle Loop Environment

Figure 29 is a schematic of the Brayton cycle with typical working fluid (argon) temperatures indicated. The approximate loop transit time is 0.5 second.

A bleed is removed from the compressor exit to purge the seals between the working fluid and the bearing compartments. The portion of the bleed which enters the bearing compartment is purified and returned to the compressor inlet.

During normal operation a small quantity of oil will be present in the bleed return. The objective of this study was to determine the allowable oil concentration of this stream. Oil may enter the system through other means such as failure of the purification system. However, the consideration of oil contamination by abnormal operating conditions was not included in this study.

2. Lubricants Investigated

a. MIL-L-7808C

MIL-L-7808C is the least stable of the oils considered in this study. The base stock is di (2-ethyl hexyl) sebacate. Additives present in the oil are oxidation inhibitor, corrosion inhibitor, anti-foaming agent, and a load-carrying additive. Properties of the oil can be found in References 2 through 9.

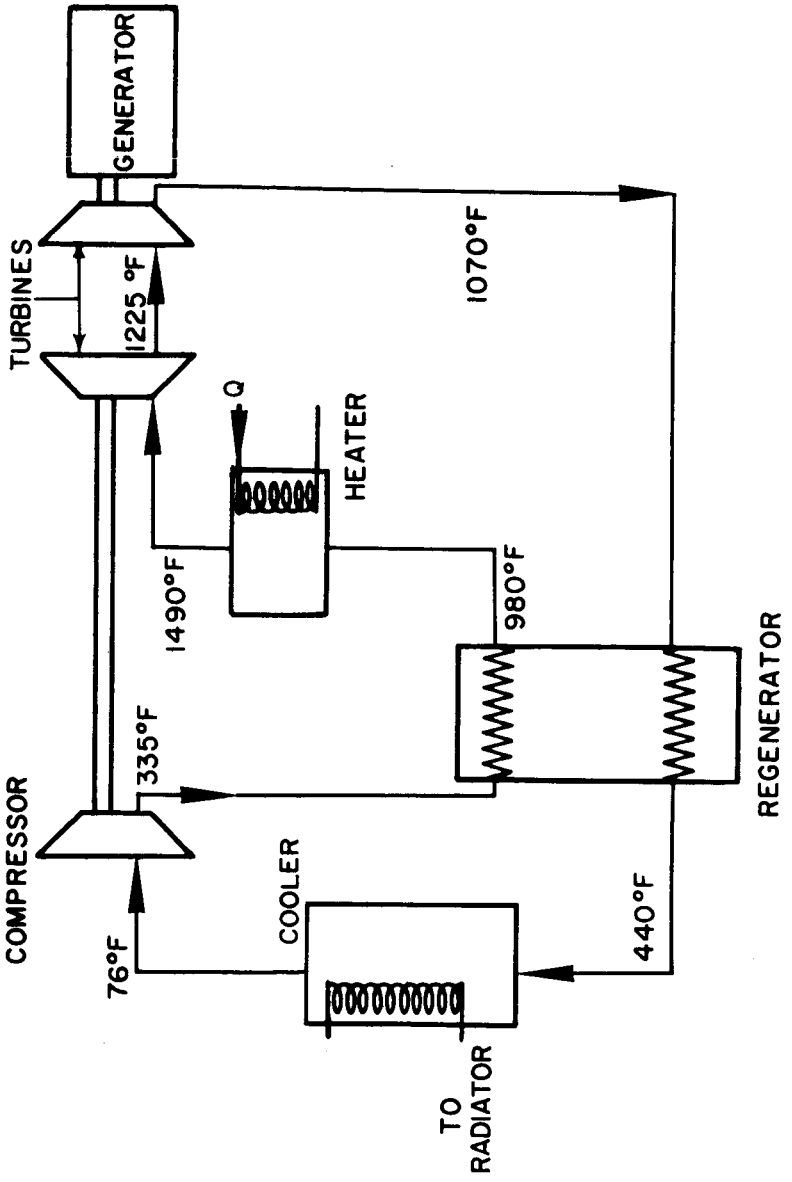

Figure 29 Schematic of Brayton Cycle with Typical Working Fluid Temperatures

b. Super-Refined Mineral Oil (MLO-7277 or 7234)

The second most stable oil considered in this study is a super-refined mineral oil. In the refining process all components containing oxygen and nitrogen, aromatics and waxes are removed. The removal of oxygen-containing impurities improves the thermal stability of the oil. Dewaxing gives lower viscosities at low temperatures. Oxidation inhibitors and anti-wear agents are added to the oil. Properties of the lubricant are given in References 4 and 10.

c. Polyphenyl Ethers

The most stable lubricants considered for the study are the polyphenyl ethers. PWA-524 is a five-ring ether (5P4E) which was developed for a jet engine application, the usual additive being an antioxidant (Reference11). Consideration is also being given to four-ring ether products (4P3E) produced by Monsanto Chemical, MCS-210 and MCS-333. These products differ in the relative abundance of the various isomers of the ether. The four-ring ethers are considered because of their lower pour point. Properties of the various polyphenyl ethers are found in References 2, 3, 4, 5, 6, 11, 12, 13, 14, 15, and 16.

B. Investigations

1. Literature Search

The major sources of data for this study are the literature. The synthetic lubricants have applications in both the aerospace and nuclear fields. References for literature on the oils can be found in Chemical Abstracts, NASA Index, and the Nucleonics Abstracts. The earliest references date back to 1950 for the aliphatic esters and 1956 for the polyphenyl ethers.

The initial investigation was made in the area of the kinetics and products from the pyrolysis of the various candidate oils. The data were found to deal only with the initial decomposition of the oil and tests were conducted at conditions appreciably different from those in the Brayton cycle.

Further investigation was made into the pyrolysis of related chemical compounds and the general theory of pyrolysis of organic chemicals.

Much early work was done in the pyrolysis of petroleum, methane, and coal, which are important reactions in industrial processes. Much recent work has been done to correlate chemical structure with thermal stability in the search for high-temperature lubricants and heat-transfer fluids.

A brief investigation was made of closed Brayton-cycle systems for stationary, marine, and space powerplants and also of gas-cooled reactor systems. It was hoped that some information would be found relating to the oil contamination problem. Apparently the practice is to tolerate some loss of coolant through seals and to locate the bearings outside of the working fluid environment, thereby avoiding the oil contamination problem.

2. Fundamental Chemistry of Pyrolysis Reactions

Pyrolysis is defined as the changes resulting from the thermal decomposition of a substance in the absence of oxygen or water. For simple substances the decomposition products may recombine to form the original substance, in which case the reaction is called reversible. With few exceptions, the complex structure of organic compounds and the large number of possible pyrolysis products makes the pyrolysis of organics irreversible.

Thermal decomposition temperatures for simple substances are specified for a given decomposition pressure. However, for irreversible reactions, the decomposition temperature usually corresponds to a given reaction rate, for example 0.1 per cent decomposition per hour.

Decomposition or pyrolysis reactions are typically first-order reactions (Reference 17) and therefore the rate of disappearance of the substance is given by Equation (1). First order reaction rates are independent of pressure. Reference 18 indicates that, for a number of organic compounds tested, the decomposition rate is lower for the gas phase pyrolysis than for the pyrolysis of the liquid.

$$dN/d\theta = -kN \qquad (1)$$

where N = moles of reacting substance
θ = time
k = reaction rate constant

The reaction rate constant is given by Equation (2). The activation energy E is a measure of the minimum energy required by the molecule to bring about the given reaction.

$$k = Ae^{-E/RT} \qquad (2)$$

where E = activation energy
R = gas constant
T = absolute temperature

A number of types of reactions occur during pyrolysis. These reactions are classed as 1) internal rearrangements, 2) bond-breaking, and 3) polymer formation.

Internal rearrangement reactions occur in organic molecules where the particular structure allows lower energy transitions or rearrangements in the structure. Compounds in which this change is irreversible exhibit poor thermal stability because of the ease of the transition.

Bond-breaking reactions, as the name implies, are reactions in which interatom bonds in molecules break. The fragments may remain for some time as free radicals which then react with other molecules. Alternatively, the fragments may undergo internal conversions to a more stable configuration. Typical products of this internal rearrangement are unsaturated hydrocarbons.

Activation energies for bond breaking are usually equal or slightly less than the bonding energies. This being the case, the weaker bonds (those with the lower bonding energy) will break at faster rates than the stronger bonds (Reference 19). The bonding energies for various interatomic bonds are given in the table below. Typical bond-breaking reactions are cracking, dehydrogenation, aromatization, and decarboxylization.

TABLE 2

Summary of Bonding Energies*

Bond	Energy, kcal/gm atom
C - C	58.6
C - O	70.0
C - H	87.3
C = C	100.0
O - H	110.2
C = O(CH_2O)	142.0

*Data from Reference 20

The benzene ring structure found in aromatic compounds is more stable than the bonding energies would indicate. This structure has an additional energy of 39 kcal/gm mole due to resonance.

One of the products usually obtained from the pyrolysis of hydrocarbons is a coke or tar-like material. This material is a high molecular weight (polymer), highly condensed substance. A number of reactions could be responsible for the polymer formation such as polymerization, condensation, or the fusion of free radicals formed by cracking.

There is evidence that tar formation results from reactions involving the initial decomposition products and not the original lubricant. In the pyrolysis of liquid diphenyl, for example, volatile products such as benzene were formed first and the insoluble polymer did not appear until some time after (Reference 5).

It appears that two competing reactions occur after the initial decomposition. The reactions are tar formation and the further degradation of products to carbon, hydrogen, and low molecular weight hydrocarbons. The relative rates of these two reactions probably depends upon temperature and the concentration of the reactants. In addition, metal surfaces in the system may have a catalytic effect upon the reactions.

3. Pyrolysis Data for Oils and Related Compounds

a. MIL-L-7808C

On the basis of bond energies, the base stock of MIL-L-7808C should begin decomposition by cracking at temperatures around 600°F. However, kinetic data indicate appreciably lower activation energies and lower decomposition temperatures. An internal rearrangement mechanism involving the carboxyl group in the ester is suspected. Decomposition begins at 520°F.

The mechanism given by the equation below has been postulated to account for the initial decomposition (pyrolysis) of the ester (References 4 and 6). There is evidence to support this mechanism. Esters were prepared with the beta hydrogen replaced by a radical which theoretically should be incapable of decomposing by the postulated mechamism. These esters were found experimentally to have a higher thermal stability.

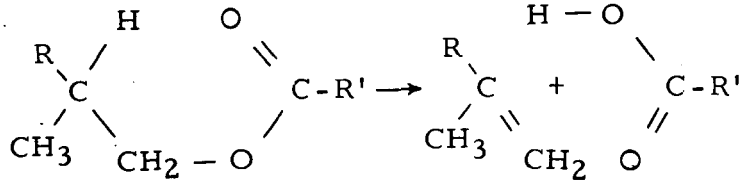

Aliphatic hydrocarbons are known to decompose by bond-breaking reactions in the temperature range of 600° to 700°F. The major reaction is cracking, which yields lighter hydrocarbons, with some dehydrogenation also occurring. Some heavier hydrocarbons and polymer (very high molecular weight species) are formed by reactions involving the initial decomposition products. Extensive dehydrogenation will yield some carbon. These same reactions are expected from the MIL-L-7808C lubricant in this temperature range.

One test in which MIL-L-7808C oil was decomposed at 635°F gave the following products: 16 per cent gas, 23 per cent carbon, and 61 per cent nonvolatile.

At higher temperatures further dehydrogenation, with more carbon, hydrogen, and polymer formation, are indicated. The gaseous products will contain more hydrogen, some methane, and only traces of other hydrocarbons. Of course, carbon monoxide, carbone dioxide, and water will be present to some extent due to the oxygen content of the ester. Methane requires temperatures of the order of 1600° to 1800°F to dehydrogenate, whereas hydrocarbons between ethane and butane dehydrogenate at approximately 1100°F.

b. MLO-7277 Mineral Oil

MLO-7277 is a highly refined mineral oil from which all traces of oxygen and nitrogen-containing compounds are removed. The manufacturer claims that the oil will not decompose until temperatures are reached where cracking of the oil occurs.

Decomposition data for a pure aliphatic hydrocarbon indicated a pyrolysis temperature of 600°F (0.1 per cent decomposition per hour). At higher temperatures the pyrolysis of this oil should proceed in a similar manner to that of MIL-L-7808C lubricant. The difference will be that no oxygen-containing compounds, such as water and carbon monoxide, will be obtained in the MLO-7277 pyrolysis products.

c. Polyphenyl Ethers

Polyphenyl ethers are expected to break down initially by the rupture of the carbon-oxygen bond in the ether linkage. This being the case, we would expect the following products from the pyrolysis of diphenyl: benzene, phenol, higher phenyl ethers, phenolic compounds, polyphenyls, and polymer. In a test where diphenyl ether was irradiated (not pyrolysed), all of these compounds were found except the polyphenyls. Also, appreciably less benzene than phenol was found in the products. It is difficult to say what became of the phenyl half of the ether after fission; the reference is vague on this question. Possible explanations are 1) oxidation of benzene by traces of impurities, or 2) the phenyl groups were consumed in polymer formation. As expected, the gas yield, principally hydrogen, was quite small. Also, little evidence of fission of benzene rings was found.

A four-ring ether was decomposed in a helium atmosphere at 650°C (1202°F) in a bomb test. Approximately equal quantities of benzene, phenol, and diphenyl ether were formed, plus a small quantity of hydrogen. These products indicate random breaking and recombining of the ether bonds.

A four-ring ether, bis (p-phenoxyphenyl) ether, was heated for 10 hours at 900°F (References 11 and 6). Only 31.5 per cent of the original ether remained after the test. The gas release was quite small, 1.7 ml per gram of oil. The gaseous products were chiefly carbon monoxide, hydrogen, carbon dioxide and methane. Small amounts of water, benzene, and light aliphatic hydrocarbons (other than methane) were present in the gas products. The major decomposition products are light liquid 27.3 per cent, unchanged ether 31.5 per cent, and heavy ends 41.2 per cent. The composition of the light liquid product is given in the following table. These products appear to be what one would expect from random breaking of the ether linkages. The heavy ends, containing products with a higher molecular weight, were not analyzed.

TABLE 3

Composition of Light Liquid Fraction,	Weight %
benzene and phenol	21.6
phenyl ether	18.3
m-phenoxyphenol	17.9
m-diphenoxybenzene	24.5
m(m-phenoxyphenoxy) phenol	8.1
unidentified products	10.3

At higher temperatures the dehydrogenation of the oil is expected. Benzene for example, yields hydrogen, biphenyl, and small amounts of terphenyl when heated to temperatures in the range of 500 to 750°C (930-1380°F). Above 750°C more extensive dehydrogenation occurs, yielding hydrogen and carbon (Reference 21).

Dowtherm A (~75 per cent diphenyl ether) and various polyphenyls were subjected to temperatures of 1000°F (Reference 5). These materials, being aromatic compounds without aliphatic side chains, are related compounds to the polyphenyl ethers and may be expected

to exhibit similar reactions in pyrolysis. After 28 hours of exposure to 1000°F all of these materials reverted to coke with less than one mole of hydrogen released per mole of starting compound. The coke was not carbon but a highly-condensed polyaromatic compound.

Other pyrolysis tests (Reference 22) with polyaromatic compounds at temperatures to 450°C (840°F) yielded primarily high boiling compounds with a small release of hydrogen and methane.

Reference 19 indicates that during the last phase of the production of coke, which consists of heating the semicoke from 1100°F to 1500°F, the following reactions occur: 1) loss of hydrogen and other gases, 2) hydrogenation of phenolic compounds yielding water and hydrocarbons, and 3) formation of higher aromatics from the semicoke.

4. Investigation of Kinetics of Pyrolysis Reactions

A study was made of the kinetics of the decomposition of oils to determine at what point in the Brayton cycle the major decomposition of oils occurs.

The constant A and the activation energy E were determined by fitting Equation (2) to the kinetic data. The units of A are reciprocal hours. The results are given in Table 4.

TABLE 4

Summary of Kinetics Study Results

Oil	E, kcal/mole	ln A	Decomposition Temp., °F		Max. Rate Temp., °F
sebacate ester	41.5	31.7	k=0.1%/hr	516	1530
hydrocarbon	49.7	35.8		596	1520
polyphenyl ether (4-ring)	63.7	38.6		810	1790

It was assumed that the working fluid and oil vapor was heated at a

constant rate. The temperature is given by Equation (3), where B is the heating rate.

$$T = B\theta \tag{3}$$

The exact solution of the kinetics equations is difficult. However, it is relatively simple to solve for the time and temperature for which the rate of decomposition ($-dN/d\theta$) is a maximum. This temperature will indicate at what point in the cycle most of the oil is decomposing. If the computed temperature is higher than the maximum loop temperature, we may conclude the following: 1) some oil may survive the first pass through the heater, and 2) the maximum decomposition will occur at the hottest part of the cycle. If the temperature is less than the maximum in the loop, we conclude 1) most of the oil is decomposed in the first pass through the heater, and 2) maximum decomposition occurs at the computed temperature.

The maximum rate temperature is found by setting $d^2N/d\theta^2$ equal to zero. The result is given by Equation (4). The maximum rate temperatures for the various oils are given in Table 4 for a heating rate of 10,000°F per second.

$$k = EB/RT^2 \tag{4}$$

The kinetics study indicates that 1) the maximum decomposition for a heating rate of 10,000°F/sec occurs at an appreciably higher temperature than the usually quoted decomposition temperature which corresponds to 0.1 per cent per hour, and 2) all of the oils studied will decompose in the hottest part of the heater.

These results came from an extrapolation of the data for the initial decomposition reactions. There is no data that would allow the determination of the temperature at which polymer or coke formation occurs. Also, at these high temperatures the initial decomposition may occur by a different reaction than the one which predominates at the lower temperatures.

5. Effects of Decomposition Products on Brayton-Cycle Performance

The consequences of oil contamination of the Brayton cycle are not known. However, some indication of the tolerances for oil con-

tamination can be obtained by assuming alternate kinds and distributions of pyrolysis products and deducing the consequences on system performance.

Two alternate problems were examined: 1) what happens if the oil condenses uniformly in the cooler, and 2) what happens if the oil cokes uniformly in the heater with complete evolution of hydrogen.

The following data were assumed for the cooler:

heat transfer coefficient U	= 4 Btu/ft^2 hr °F
hydraulic diameter	= 0.1 inch
heat input Q	= 102,700 Btu/hr
log mean temperature difference	= 55.2 °F
$\Delta p/p$	= 0.07

The oil film thickness was computed which gives a rise in $\Delta p/p$ of 0.02; this would reduce the overall cycle efficiency by 1.3 per cent. Assuming laminar flow in the cooler, the film thickness was 0.00305 inch. The computed cooler surface is 464 ft^2 and the oil density (solid polyphenyl ether) is estimated to be 62 lbs/ft^3. The oil weight deduced from this data is 7.3 lbs.

The effect of this deposit on the cooler heat transfer was computed. The conductivity of liquid polyphenyl ether was used (0.075 Btu/ft hr °F). The 7.3 pounds of oil will lower the heat transfer coefficient U by 0.05 Btu/hr °F ft^2, a small change. The effect of the flow change, due to the increased $\Delta p/p$, on heat transfer was not computed.

Analysis of the heater was performed and the quantity of coke required to produce a $\Delta p/p$ of 0.02 was deduced. Pertinent heater data are given below:

heat transfer surface	= 208 ft^2
hydraulic diameter	= 0.18 inch
$\Delta p/p$	= 0.0272

Assuming laminar flow, uniform deposit, and a density of 90 lbs/ft^3, a coke weight of 9.0 lbs was obtained to produce a loss in cycle efficiency of about 1.3 per cent. The effect of the uniform coke deposit on heat transfer in the heater is quite small. Estimated conductivity of the coke is 2.9 Btu/ft hr °F (Perry's Handbook).

The maximum hydrogen and carbon monoxide release from the oils can be estimated from the compositions given in Table 5. Probably the molecular sieve can be counted on to remove carbon monoxide so that only hydrogen release to the argon needs to be considered.

TABLE 5

Theoretical Chemical Compositions of Lubricants

Oil	C	H	O	Mol. wt.
dioctyl sebacate ester	73.3	11.7	15.0	426
naphthenic hydrocarbon (C_nH_{2n})	85.7	14.3	0.0	-
4-ring polyphenyl ether	81.3	5.1	13.6	354

An analysis was performed of the effects of hydrogen addition to the cycle. The compressor inlet temperature was considered to be a constant and the total heat addition to the cycle was considered a constant. Also, some method of pressure relief was assumed, such that the compressor inlet pressure was maintained at the design value. The increase in specific heat of the working fluid with hydrogen contamination results in a decrease in heater exit temperature and a corresponding decrease in cycle efficiency and power output. Figure 30 indicates the effects of hydrogen contamination on the turbine inlet temperature, the gross power output and the turbine-compressor rotational speed. Since a constant heat input was assumed, the cycle efficiency is proportional to gross power output. The calculations extend to hydrogen contaminations up to 0.004 lb. Although the maximum tolerable contamination has not been determined, it is probably somewhat above 0.005 lb of hydrogen. Greater hydrogen contamination will reduce the turbine inlet temperature sufficiently to result in a non-self-sustaining cycle.

Evidently, it is important to remove the hydrogen from the system as it is evolved. Many metals will permit hydrogen to diffuse when maintained at a proper temperature. Palladium is often selected for this type of application. Perhaps a palladium window should be included in the basic powerplant to eliminate hydrogen from the cycle.

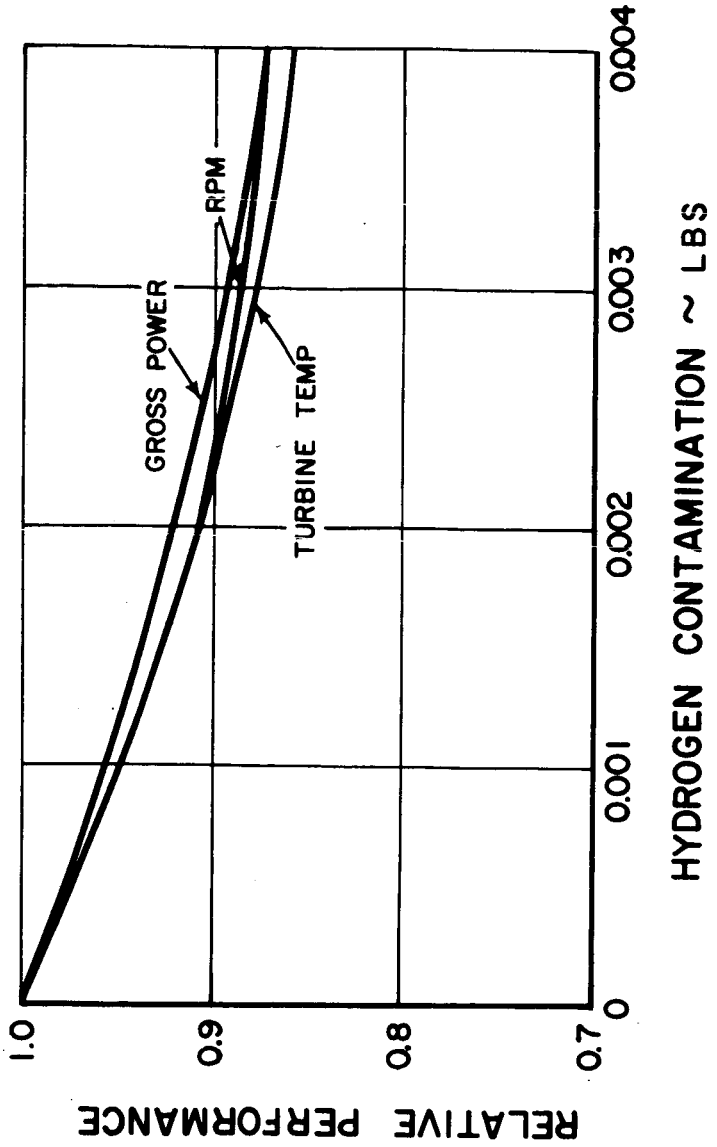

Figure 30 Effect of Hydrogen Addition on System Performance

C. Results

The pertinent data presented in Section B above are insufficient to determine with certainty the consequences of oil contamination of the Brayton-cycle working fluid. This section will give the best estimate as to the consequences of oil contamination based on the available information. It must be understood that some of the results are conjectural and therefore may require revision as new data become available.

The composition and distribution of products of oil pyrolysis are determined by transport and chemical kinetics considerations. The initial decomposition of oils will occur in the small fraction of a second the vapor makes the first pass through the heater. The coking and hydrogen evolution from deposits in the heater will occur over periods of the order of months. Reactions which occur over the period of the order of minutes are not important for the following reasons: 1) the loop has a very small transit time, and 2) the hot end of the loop is at a high enough temperature so that pyrolysis reactions are quite rapid.

1. MIL-L-7808C (Sebacate Ester)

The kinetic data indicate that the sebacate ester oil will decompose at the hot end of the loop where temperatures are in the range of 1400 to 1500°F. The initial deposits will be a mixture of carbon and polymer. The relative amounts of carbon and polymer depend upon the relative rates of the cracking and polymer-forming reactions. However, in time the deposits will coke and evolve hydrogen so that the final products will be carbon deposits in any case.

Gaseous products will be chiefly hydrogen, carbon dioxide, carbon monoxide, and methane. All of these products except hydrogen will be continually removed by the molecular sieve in the bleed purification system. Hydrogen gas will accumulate in the working fluid.

Some low vapor pressure products may pass through the cooler. However, the concentration of these products will probably be too low for them to condense (their partial pressure will be less than the vapor pressure of the liquid).

In summary, the products of the pyrolysis of MIL-L-7808C in the Brayton cycle are, 1) a nonuniform deposit of coke in the heater (greatest deposit in the hot end), 2) an accumulation of hydrogen in the working fluid, and 3) the absorption of methane, carbon monoxide, and carbon dioxide in the molecular sieve.

2. Refined Mineral Oil (Hydrocarbon Oil)

The results of the pyrolysis of the mineral oil in the Brayton-cycle loop are expected to be similar to those of the pyrolysis of MIL-L-7808C. The results are 1) accumulation of coke in the hot end of the heater, 2) accumulation of hydrogen in the working fluid, and 3) the absorption of methane by the molecular sieve. The hydrocarbon oil will yield more hydrogen than the MIL-L-7808C and will give no products containing oxygen (unless additives contain oxygen).

3. Polyphenyl Ethers

Kinetic studies indicate that the maximum rate of decomposition of the polyphenyl ether will occur in the hottest part of the heater. There is some conflicting data that is judged to be in error, which indicates maximum decomposition at 1100°F.

The polyphenyl ether is expected to survive several passes through the heater with some tar deposition occurring each pass. Coking, with hydrogen evolution, will occur in the tar deposits at a slower rate than with the other lubricants studied. The extent of coking is not known, but is judged to not be appreciable at temperatures below 1400°F.

To summarize, the expected products from the pyrolysis of polyphenyl ether are (1) tar deposition chiefly in the hottest section of the heater, (2) gradual coking of the deposits (extent unknown) with hydrogen evolution, (3) light weight compounds such as benzene, phenol, and phenyl ether evolved and being removed by the adsorber, and (4) possible condensation of lower volatility products in the cooler part of the loop.

APPENDIX 2

References

APPENDIX 2

References

1. Kannel, J., J. C. Bell and J. A. Walowit, Battelle Memorial Institute, Rept. ASD TDR 61-643, Part V, A Study of the Influence of Lubricants on High-Speed Rolling-Contact Bearing Performance

2. Adamczak, R. L., R. J. Benzing, and H. Schwenker, Advanced Lubricants and Lubrication Techniques, Ind. and Eng. Chem., Vol. 56, No. 1, 1964

3. Bisson, E. E., and W. J. Anderson, (eds), Advanced Bearing Technology, NASA SP-38

4. Blake, E. S., et al, Thermal Stability as a Function of Chemical Structure, Journal of Chem. and Engr. Data, Vol. 6, No. 1, 1961

5. Bolt and Carroll, Radiation Effects on Organic Materials, Academic Press

6. Gunderson and Hart (eds), Synthetic Lubricants, Reinhold Publishing Company

7. Larsen, R. G. and A. Bondi, Functional Selection of Synthetic Lubricants, Ind. and Eng. Chem., Vol. 42, No. 12, 1950

8. McTurk, W. E., et al, Synthetic Lubricants, WADC, AF Tech. Report 6663, 1951

9. Boeing Report, Document D-14766-8, 1953

10. Super-Refined Hydraulic Oils, Bulletin D237-E, Humble Oil and Refining Company

11. Groth, R. H., Polyphenyl Ethers, PWA memo, 12/17/63

12. Mahoney, C. L., et al, Engine Oil Development, WADC TR-57-177, Part II

13. Mahoney, C. L., et al, Nuclear Radiation Resistant High Temperature Lubricants, WADC TR 59-173

14. Mahoney, C. L., et al, Polyphenyl Ethers as High-Temperature Radiation-Resistant Lubricants, Journal of Chem. and Engr. Data, Vol. 5, No. 2, 1960

15. Rice, W. L. R., D. A. Kirk, and W. B. Cheney, Radiation-Resistant Fluids and Lubricants, Nucleonics, Vol. 18, No. 2, 1960

16. Schmidt-Collerus, and Bohner, Determination of the Relation Between Structure and Radiation Stability of Aryl Ether Fluids, WADD TR 60-282

17. Frost and Pearson, Kinetics and Mechanism, 2nd ed., John Wiley and Sons

18. Johns, I. B., E. A. McElhill, and S. O. Smith, Thermal Stability of Organic Compounds, I and EC Product Research and Dev., Vol. 1, No. 1, 1962

19. Fuchs, W., and A. G. Sandhoff, Theory of Coal Pyrolysis, Ind. and Eng. Chem., Vol. 34, No. 5, 1942

20. Fieser and Fieser, Organic Chemistry, 3rd ed., Reinhold Publishing Company

21. Othmer, Encyclopedia of Chemical Technology

22. Weiss, Jr., et al, Radiolysis and Pyrolysis of Polyaromatic Compounds, I & EC Product Research and Dev., Vol. 3, No. 2, 1964

Distribution List
Contract NAS3-7635

To	No. of Copies
National Aeronautics and Space Administration Lewis Research Center 21000 Brookpark Road Cleveland, Ohio 44135	
Attention: B. Lubarsky, MS 500-201	1
I. Pinkel, MS 5-3	1
R. L. Cummings, MS 500-201	1
J. Heller, MS 500-201	1
W. Stewart, MS 5-9	1
D. C. Guentert, MS 500-201	1
J. E. Dilley, MS 500-309	1
W. J. Anderson, MS 6-1	1
Z. Nemeth, MS 6-1	1
E. Zaretsky, MS 49-1	1
R. L. Johnson, MS 5-8	1
L. P. Ludwig, MS 5-8	1
H. Rohlik, MS 6-1	1
B. Wong, MS 6-1	1
A. Straquadine, MS 500-203	1
L. W. Ream, MS 500-201	1
Technology Utilization Office, MS 3-19	1
Librarian	1
National Aeronautics and Space Administration Washington, D. C. 20546	
Attention: T. C. Evans, MTF	1
F. P. Dixon, MTG	1
A. M. Andrus, ST	1
H. Rochen, RN	1
J. J. Lynch, RNP	1
National Aeronautics and Space Administration Scientific and Technical Information Facility P. O. Box 33, College Park, Maryland 20740	
Attention: Acquisitions Branch, SQT-34054	2+ repro
National Aeronautics and Space Administration Goddard Space Flight Center Greenbelt, Maryland 20771	
Attention: W. R. Cherry	1
Librarian	1
National Aeronautics and Space Administration Langley Research Center Langley Station, Hampton, Virginia 23365	
Attention: R. C. Wells	1
Librarian	1
National Aeronautics and Space Administration George C. Marshall Space Flight Center Huntsville, Alabama 35812	
Attention: E. Stuhlinger	1
Librarian	1
National Aeronautics and Space Administration Manned Spacecraft Center Houston, Texas 77058	
Attention: R. B. Ferguson	1
Librarian	1
National Aeronautics and Space Administration Jet Propulsion Laboratory 4800 Oak Grove Drive Pasadena, California 91103	
Attention: J. W. Goldsmith	1
Librarian	1
National Aeronautics and Space Administration Ames Research Center Moffett Field, California 94035	
Attention: Librarian	1
Electronic Research Center 575 Technology Square Cambridge, Massachusetts, 02139	
Attention: Librarian	1

To:	No. of Copies
U.S. Atomic Energy Commission, DRD Washington, D.C. 20454	
Attention: N. Grossman	1
J. LaScalzo	1
R. Oehl	1
D. B. Hoatson, ARB	1
Librarian	1
U. S. Atomic Energy Commission Technical Information Extension P. O. Box 62, Oak Ridge, Tennessee 37831	
Attention: Librarian	1
U. S. Atomic Energy Commission Argonne National Laboratory 9700 South Cass Avenue Argonne, Illinois 60440	
Attention: Librarian	1
U. S. Army Engineer R&D Laboratories Gas Turbine Test Facility Fort Belvoir, Virginia 22060	
Attention: W. Crim	1
Department of the Navy Office of Naval Research Washington, D. C. 20360	
Attention: Dr. R. Roberts	1
Department of the Navy Bureau of Naval Weapons Washington 25, D.C.	
Attention: Code RAPP	1
Department of the Navy Bureau of Ships Washington 25, D. C.	
Attention: G. L. Graves	1
Department of the Navy Naval Research Laboratory Washington, D. C. 20390	
Attention: Librarian	1
Air Force Systems Command Aeronautical Systems Division Wright-Patterson AFB, Ohio 45433	
Attention: G. W. Sherman, APIP	1
Librarian	1
National Bureau of Standards Washington 25, D. C.	
Attention: Librarian	1
Massachusetts Institute of Technology Cambridge, Massachusetts 02139	
Attention: Librarian	1
University of Pennsylvania Power Information Center, Moore School Building 200 South 33rd Street Philadelphia, Pennsulvania 19104	1
Battelle-Northwest P. O. Box 999, Richland, Washington 99352	
Attention: Librarian	1
Institute for Defense Analyses 400 Army Navy Drive Arlington, Virginia 22202	
Attention: Librarian	1
The Franklin Institute Benjamin Franklin Parkway at 20th Street Philadelphia, Pennsylvania 19103	
Attention: Librarian	1

To:	No. of Copies
The Rand Corporation 1700 Main Street Santa Monica, California Attention: Librarian	1
Williams Research Walled Lake, Michigan Attention: Librarian	1
Aerojet-General Coporation Azusa, California 91703 Attention: Librarian	1
Aerojet-General Nucleonics San Ramon, California 94583 Attention: Librarian	1
AiResearch Manufacturing Company A Division of the Garrett Corporation Phoenix, Arizona 85034 Attention: Librarian	1
AiResearch Manufacturing Company A Division of the Garrett Corporation 9851 Sepulveda Boulevard Los Angeles, California 90009 Attention: Librarian	1
Avco Rand Corporation 201 Lowell Street Wilmington, Massachusetts Attention: Librarian	1
Chrysler Corporation Space Division, Technical Information Center P. O. Box 26018, New Orleans, Louisiana 70126 Attention: Librarian	1
Douglas Aircraft Company 3000 Ocean Park Boulevard Santa Monica, California Attention: Librarian	1
Electro-Optical Systems, Inc. 300 North Halstead Avenue Pasadena, California 91107 Attention: Librarian	1
Fairchild Hiller Republic Aviation Division Farmingdale, Long Island, New York 11735 Attention: Librarian	1
General Dynamics Corporation General Atomic Division San Diego, California Attention: Librarian 92112	1
General Electric Company Flight Propulsion Laboratory Department Cincinnati, Ohio 45215 Attention: Librarian	1
General Electric Company Lynn, Massachusetts Attention: Librarian	1
General Electric Company Missile and Space Vehicle Department 3198 Chestnut Street Philadelphia, Pennsylvania 19104 Attention: Librarian	1
Lockheed Aircraft Corporation Missiles & Space Division P. O. Box 504, Sunnyvale, California Attention: Librarian	1

To:	No. of Copies
Martin Company, Baltimore Division Martin-Marietta Corporation P. O. Box 5042, Baltimore, Maryland 21203 Attention: Librarian	1
Mechanical Technology Incorporated 968 Albany-Shaker Road Latham, New York 12110 Attention: Librarian	1
North American Aviation, Inc. Atomics International Division 8900 DeSoto Avenue Canoga Park, California Attention: Librarian	1
North American Aviation, Inc. Space and Information Systems Division Downey, California 90241 Attention: Librarian	1
Philco Corporation, Aeronutronic Division Ford Road, Newport Beach, California 92663 Attention: Librarian	1
Solar 2200 Pacific Highway San Diego, California 92112 Attention: Librarian	1
Space General Corporation 9200 East Flair Drive El Monte, California Attention: Librarian	1
Space Technology Laboratories, Inc. One Space Park Redondo Beach, California Attention: Librarian	1
*Sunstrand Aviation 2480 West 70th Avenue Denver, Colorado 80221 Attention: Librarian	1
S. V. Manson & Company, Inc. 2420 Wilson Boulevard Arlington, Virginia 22201 Attention: Librarian	1
The Bendix Corporation Research Laboratories Division Southfield, Michigan Attention: Librarian	1
The Boeing Company Aero-Space Division P. O. Box 307, Seattle 25, Washington Attention: Librarian	1
TRW, Inc. 7209 Platt Avenue Cleveland, Ohio 44104 Attention: Librarian	1
Union Carbide Corporation Linde Division 61 East Park Drive, Tonowanda, New York Attention: Librarian	1
United Aircraft Corporation Research Laboratories East Hartford, Connecticut 06108 Attention: Librarian	1
Westinghouse Electric Corporation Astronuclear Laboratory P. O. Box 10864 Pittsburgh, Pennsylvania 15236 Attention: Librarian	1